

A THEORETICAL AND EXPERIMENTAL INVESTIGATION OF ENERGY-CONTAINING SCALES IN THE DYNAMIC SUBLAYER OF BOUNDARY-LAYER FLOWS

GABRIEL KATUL^{1,2} and CHIA-REN CHU³

¹*School of the Environment, Box 90328, Duke University, Durham, North Carolina 27708-0328, U.S.A.;* ²*Center for Hydrologic Sciences, Duke University, Durham, North Carolina 27708, U.S.A.;* ³*Department of Civil Engineering, National Central University, Chung-Li, Taiwan*

(Received in final form 20 August, 1997)

Abstract. The existence of universal power laws at low wavenumbers (K) in the energy spectrum (E_u) of the turbulent longitudinal velocity (u) is examined theoretically and experimentally for the near-neutral atmospheric surface layer. Newly derived power-law solutions to Tchen's approximate integral spectral budget equation are tested for strong- and weak-interaction cases between the mean flow and turbulent vorticity fields. To verify whether these solutions reproduce the measured E_u at low wavenumbers, velocity measurements were collected in the dynamic sublayer of the atmosphere at three sites and in the inner region of a laboratory open channel. The atmospheric surface layer measurements were carried out using triaxial sonic anemometers over tall corn, short grass, and smooth desert-like sandy soil. The open channel measurements were performed using a two-dimensional boundary-layer probe above a smooth stainless steel bed. Comparisons between the proposed analytical solution for E_u , the dimensional analysis by Kader and Yaglom, and the measured Haar wavelet E_u spectra are presented. It is shown that when strong interaction between the mean flow and turbulent vorticity field occurs, wavelet spectra measurements, predictions by the analytical solution, and predictions by the dimensional analysis of Kader-Yaglom (KY) are all in good agreement and confirm the existence of a -1 power law in $E_u (= C_{uu} u_*^2 K^{-1}$, where C_{uu} is a constant and u_* is the friction velocity). The normalized upper wavenumber limit of the -1 power law ($Kz = 1$, where z is the height above the zero-plane displacement) is estimated using two separate approaches and compared to the open channel and atmospheric surface-layer measurements. It is demonstrated that the measured upper wavenumber limit is consistent with Tchen's budget but not with the KY assumptions. The constraints as to whether the mean flow and turbulent vorticity strongly interact are considered using a proposed analysis by Panchev. It is demonstrated that the arguments by Panchev cannot be consistent with surface-layer turbulence. Using dimensional analysis and Heisenberg's turbulent viscosity model, new constraints are proposed. The new constraints agree with the open channel and atmospheric surface-layer measurements, Townsend's 'inactive eddy motion hypothesis', and the Perry et al. analysis.

1. Introduction

It is recognized that turbulent eddy motion in the atmospheric boundary layer (ABL) exhibits three spectral regions (see e.g., Kaimal and Finnigan, 1994; Sorbjan, 1989): (1) The *energy containing range* (or large-scale turbulence), in which turbulent kinetic energy per unit mass (TKE) is produced, (2) the *inertial subrange* (or small scale turbulence), in which TKE is neither produced nor dissipated, but is simply transported from large to small scales, and (3) the *dissipation range*, where TKE is converted to internal energy by the action of fluid viscosity. While much effort has been devoted to investigating the inertial subrange following the success of

Kolmogorov's (1941) theory (hereafter referred to as K41) and other refinements (see Wang et al., 1996; Frisch, 1995), less attention was devoted to the spectral characteristics of the energy containing range despite their importance in mass, energy, and momentum transport. Interest in the inertial subrange is driven, in part, by possible theoretical simplifications to the flow equations using local isotropy assumptions and independence from boundary conditions (Monin and Yaglom, 1975), and the extensive scales (2 to 3 decades) over which inertial subrange signatures (e.g., $-5/3$ power law) have been reported both in ABL and laboratory experiments. In contrast, the analysis of large-scale turbulence is a far more complex task than that of describing the inertial or dissipation scales because of their strong anisotropy and their dependence on the flow domain boundary properties.

Despite the complexity associated with analysis of large-scale turbulence, several laboratory and field experiments in Table I reported well-defined -1 power laws at production scales for the longitudinal velocity spectrum in the dynamic sublayer (DSL) of many boundary-layer flows. Theoretical and phenomenological analyses to explain occurrences of the -1 power law resulted in three approaches: (1) Townsend's (1976) attached eddy hypothesis, which was successfully used by Perry and Abell (1975, 1977), Perry and Chong (1982), Perry et al. (1986, 1987, 1994), and Perry and Li (1986, 1990) to describe the longitudinal (E_u) and vertical velocity (E_w) power spectra at low wavenumbers (K) for many pipe and plate boundary-layer flows, (2) the dimensional analysis proposed by Kader and Yaglom (1984, 1991) for the DSL of the atmosphere, and (3) Tchen's (1953, 1954) and Panchev's (1969, 1971) theoretical analyses of an approximate spectral budget for E_u . While the emergence of a -1 power law at low wavenumbers for the E_u spectrum has been reported in many laboratory experiments as evidenced by Table I, its existence and onset in the atmospheric surface layer (ASL) remains questionable as noted by the theoretical study of Claussen (1985), the review by Raupach et al. (1991), and the discussion by Antonia and Raupach (1993). This uncertainty is attributed to the absence of a -1 power law in the measured velocity spectra from the Kansas (see Kaimal et al., 1972) and Minnesota experiments (see Kaimal, 1978).

The possibility that energy-containing scales, governed by the dynamics of anisotropic eddy motion and possibly boundary roughness conditions (as proposed by Krogstad et al., 1992), attain a universal power-law in the DSL has been the subject of recent research (Antonia and Raupach, 1993; Yaglom, 1994; Katul et al., 1995a, 1996a). The objective is to investigate theoretically and experimentally occurrences of such power laws within the energy-containing range of E_u . Controversies regarding the onset of such power laws at production scales in the near-neutral surface layer, inconsistencies between assumptions central to the dimensional analysis of Kader and Yaglom (1984, 1991) and laboratory measurements, and the role of boundary roughness conditions are investigated theoretically and experimentally.

Table I

Sample studies reporting the occurrence of a -1 power law in the longitudinal velocity power spectrum (E_u) at low wavenumbers ($Kz < 1$), where z is the height above the zero-plane displacement

| Authors | Flow type | Comments |
|------------------------------|--|---|
| Tchen (1953, 1954) | Theoretical | Approximate asymptotic solution to the spectral budget based on Heisenberg's (1948) turbulent viscosity model. |
| Klebanoff (1954) | Flat plate boundary layer with zero-pressure gradient | -1 power law existed for $z/h_b = 0.05$ but not for $z/h_b = 0.0011$ and 0.8 (see Hinze, 1959, p. 501). |
| Hinze (1959, p. 501) | Data from Klebanoff (1954) | -1 power law occurs in regions of strong TKE production. |
| Pond et al. (1966) | ASL spectra over ocean surfaces | -1 power law existed at low wavenumbers. Note that three sensor types were used to measure the velocity spectra and all spectra measurements agreed at low wavenumbers. |
| Bremhorst and Bullock (1970) | Fully developed pipe flow | -1 power law existed at wavelengths equal to or greater than the pipe diameter. |
| Panchev (1971) | Theoretical | Prediction based on Tchen's (1953) spectral budget. |
| Bremhorst and Walker (1973) | Fully developed pipe flow | -1 power law noted in the inner region, higher frequencies responsible for the transfer of momentum from the wall into the fluid while lower frequencies contribute to the transfer of momentum from the fluid to the wall. |
| Perry and Abell (1975, 1977) | Turbulent air flow in a pipe (rough and smooth walls) | -1 power law existed at low wavenumbers in the inner region. No -1 power law was measured for E_w . |
| Korotkov (1976) | Channel flow measurements | Same as above. |
| Kaimal (1978) | ASL E_u measurements for unstable conditions from the Minnesota experiment | No -1 power law observed but low wavenumbers spectral properties are a function of mixed layer variables (see also Bradshaw's, 1978 comment on Kaimal's findings). |
| Bullock et al. (1978) | Fully developed pipe flow | -1 power law in the inner region for $z^+ (= zu_* / \eta)$ between 70 and 500. |
| Hunt and Joubert (1979) | Smooth-wall duct flow | -1 power law for $Kz < 1$ in the logarithmic region. Townsend's (1976) attached eddy hypothesis is used for interpretation. |
| Kader and Yaglom (1984) | Surface-layer turbulence | -1 power law derived from dimensional analysis and height invariance of E_u . |
| Claussen (1985) | Surface-layer turbulence | No -1 power law at low wavenumbers from arguments analogous to Panchev (1971) and the spectral budget. |
| Perry et al. (1986) | Smooth pipe flow and vortex model | -1 power law observed for $z/h_b < 0.01$ and $Kz > 1$ in E_u but not E_w . |
| Perry et al. (1987) | Smooth and rough boundary layers with zero-pressure gradient | -1 power law in E_u for both rough and smooth in the overlap region between the inner and outer flow. |

Table I
Continued

| Authors | Flow type | Comments |
|-----------------------------|--|--|
| Turan et al. (1987) | Fully developed pipe flow | -1 power law for $Kz < 1$ for pipe-flow boundary layer for zero and favorable pressure gradient. Departures are noted for adverse pressure gradient. |
| Erm et al. (1987) | Smooth flat surface with zero pressure gradient | Results similar to Perry et al. (1987) but their Reynolds number is lower by a factor of 8. |
| Perry and Li (1990) | Smooth and rough (both k -type and d -type) boundary layers with zero-pressure gradient | -1 power law in E_u observed for $Kz > 1$ and $zu_*/\eta > 100$, and $z/h_b < 0.15$. Better collapse of low-wavenumber spectra with outer flow variables. |
| Erm and Joubert (1991) | Moderate Reynolds number turbulent boundary layer over a flat smooth surface with zero pressure gradient | -1 power law observed at $z/h_b = 0.1$ but not at $z/h_b > 0.35$. |
| Antonia and Raupach (1993) | Inner region of a rough-wall laboratory boundary layer | Argued against a -1 power in the ASL based on the measured spectra from Kansas experiments (Kaimal et al., 1972). |
| Kader and Yaglom (1991) | Dynamic sublayer of the ASL | Extensive -1 power law for $Kz \leq 0.1$ for E_u . |
| Yaglom (1994) | Over-all review of dimensional analysis of spectra | -1 power law must exist for a neutral ASL. |
| Katul et al. (1995a, 1996a) | Dynamic sublayer of a sandy dry lakebed and a forest clearing | Same as Kader and Yaglom (1984, 1991) but also inactive eddy motion investigated using simultaneous free air static pressure and velocity measurements in the forest clearing (Katul et al., 1996a). |

For this purpose, approximate solutions to a theoretical integral spectral budget equation proposed by Tchen (1953, 1954) are derived and tested using high frequency (10–56 Hz) triaxial sonic anemometer velocity measurements at three sites with different momentum roughness lengths (z_0) and climatic regimes. Also, 100 Hz velocity measurements in the boundary layer of a laboratory open channel are used as bench-mark tests to investigate the proposed approximate solutions for: (i) smooth-wall boundary layers, (ii) conditions of no thermal ground inhomogeneity and negligible sensible heat flux (see Kader and Yaglom, 1990; Kader, 1992; Yaglom, 1993 for discussion), and (iii) a different fluid.

The dynamic sublayer is considered because (1) of the extensive laboratory measurements on rough and smooth-wall boundary-layer flows available for comparisons (see Table I), (2) any ASL theory developed for non-neutral stratification must match, in the limit, the neutral case, (3) near-neutral conditions frequently

exist above very rough surfaces such as forests and tall natural vegetation, and (4) the well established characteristic length and velocity scales in the DSL facilitate the estimation of length and velocity scales for less understood statistical quantities such as turbulent flow vorticity.

The notation used is as follows: U_i ($U_1 = U, U_2 = V, U_3 = W$) are the instantaneous longitudinal, lateral, and vertical velocity components along x_i ($x_1 = x, x_2 = y, \text{ and } x_3 = z$), u_i are the turbulent velocity perturbations ($\langle u_i \rangle = 0$), $\langle \rangle$ is time averaging, and $\langle U \rangle$ is aligned along the mean wind direction so that $\langle V \rangle = 0$. It is understood that z is the height above the zero-plane displacement (d) for vegetated surfaces. Both meteorological and index notations are used. Also, the terms dynamic sublayer and near-neutral atmospheric surface layer are used interchangeably for consistency with the definition by Kader and Yaglom (1990). It is assumed that the DSL is a non-thermally stratified region for which the turbulent stresses ($\langle u_i u_j \rangle$) and friction velocity (u_*) do not vary appreciably with z (i.e. $<10\%$) and $\langle U_1 \rangle$ varies logarithmically with z .

2. Theory

To determine the spectral properties of u , the energy balance for a steady-state planar homogeneous turbulence in wavenumber space as derived by Tchen (1953, 1954), Hinze (1959), and Panchev (1969, 1971), is considered. In Tchen's (1953) analysis, the net flow of energy from large to small eddies is a constant identical to the mean turbulent kinetic energy (TKE) dissipation rate per unit fluid mass ($\langle \epsilon \rangle$). Hence,

$$\langle \epsilon \rangle = -\langle u_1 u_3 \rangle \frac{\partial \langle U_1 \rangle}{\partial x_3} \quad (1)$$

where $\langle \epsilon \rangle = 0.5 \nu (\partial u_i / \partial x_j + \partial u_j / \partial x_i)^2$ is the mean TKE dissipation rate, and ν is the kinematic viscosity. To derive the spectral budget for E_u , consider the prognostic equations for the two-point velocity covariance given by (Hinze, 1959, p. 259)

$$\frac{\partial Q_{i,i}}{\partial t} + \left(2Q_{1,3} + r_3 \frac{\partial Q_{i,i}}{\partial r_1} \right) \frac{\partial \langle U_1 \rangle}{\partial z} = S_{i,i} + 2\nu \frac{\partial^2 Q_{i,i}}{\partial r_k \partial r_k} \quad (2)$$

where

$$Q_{i,j} = \langle u_i(x_1, x_2, x_3) u_j(x'_1, x'_2, x'_3) \rangle$$

$$r_i = x_i - x'_i$$

$$S_{i,j} = \frac{\partial}{\partial r_k} \langle S_{jk,i} + S_{ik,j} \rangle$$

$$S_{i,kj} = \langle u_i(x_1, x_2, x_3) u_j(x'_1, x'_2, x'_3) u_k(x'_1, x'_2, x'_3) \rangle$$

and r_i are the separation distance vector components between points x_i and x'_i . For steady-state conditions, Fourier transforming (2), and integrating the resultant equations from zero to any arbitrary wavenumber, the dynamic equation for the energy spectrum is given by (Hinze, 1959, p. 262)

$$\begin{aligned} \langle \epsilon \rangle &\approx 2\nu \int_0^K d\theta \theta^2 E_u(\theta) - \int_0^K d\theta F(\theta) - \frac{\partial \langle U_1 \rangle}{\partial x_3} \int_K^\infty d\theta D(\theta) \\ &= P_1 + (P_2 + P_3) \end{aligned} \quad (3)$$

where, $D(K)$ is given by

$$D(K) = 2(E_{1,3})_{\text{avg}} - \left(K_1 \frac{\partial E_{i,i}}{\partial K_3} \right)_{\text{avg}} ;$$

with

$$\int_0^\infty d\theta D(\theta) = \langle u_1 u_3 \rangle. \quad (4)$$

Here, $E_{i,j}(K)$ is the spectrum function of $\langle u_i(x) u_j(x+r) \rangle$, K_1, K_2, K_3 are the directional wavenumbers corresponding to r_1, r_2 , and r_3 , and K is a scalar wavenumber applied for averaging $E_{i,j}$ over spherical surfaces with radii $r = \text{constant}$, respectively, such that (Hinze, 1959, pp. 262–263)

$$(E_{i,j})_{\text{avg}} = \frac{1}{4\pi K^2} \int \int \int dA(K) E_{i,j}(K_1, K_2, K_3) \quad (5)$$

and $F(K)$ is the three-dimensional transfer spectrum function of $\langle u_i(x)^2 u_i(x+r) \rangle$ averaged over the spherical surfaces $r = \text{constant}$ (or $K = \text{constant}$) with

$$\int_0^\infty d\theta F(\theta) = 0 \quad (6)$$

and $E_u(K)$ ($= E_{1,1}$) is the spectral density function defining the energy between K and $K + dK$. Terms P_1, P_2 , and P_3 represent the loss of energy through viscous dissipation for wavenumbers not exceeding K , the transfer of energy to wavenumbers exceeding K , and the production of energy from all wavenumbers exceeding K . In (2) and (3), we note that the pressure transport term is neglected. This simplification was investigated by Claussen (1985) and found to be valid for ASL flows.

As discussed in Hinze (1959, p. 261) and Panchev (1971, p. 220), to represent P_2 and P_3 as a function of the scalar wavenumber K , in analogy to isotropic turbulence, averaging over all directions in the wave vector space is necessary.

In order to compute $E_u(K)$ from (3), P_2 and P_3 must be related to E_u using phenomenological models. The relationships between P_2 and P_3 and E_u were derived by Tchen (1953, 1954) using a turbulent viscosity approach. A brief review of his key assumptions is presented next.

2.1. TCHEN'S (1953) ANALYSIS

From (3), the mean dissipation of TKE is due to a molecular viscous component (P_1) superimposed on a turbulent component ($P_2 + P_3$). The turbulent dissipation component is the result of momentum exchange between turbulent eddies. In order to model P_2 and P_3 , phenomenological analogies between molecular dissipation of TKE, energy extraction from large to small scales (e.g., P_2), and energy removal from the mean to turbulent flows (e.g., P_3) are developed using Heisenberg's (1948) turbulent viscosity approach.

It is recognized that for high Reynolds number flows, the total viscous dissipation rate is related to the mean squared vorticity ($\langle\omega_i\omega_i\rangle$) amplitude using

$$\langle\epsilon\rangle = \nu\langle\omega_i\omega_i\rangle = 2\nu\int_0^\infty K^2 E_u(K)dK \quad (7)$$

where ω_i is the turbulent vorticity perturbation vector (Tennekes and Lumley, 1972, p. 88). Based on Heisenberg's (1948) analogy, Tchen (1953, 1954) proposed that a turbulent dissipation component ($S_t = P_2 + P_3$) be defined by

$$\begin{aligned} S_t &= \text{turbulent viscosity} \times \text{squared vorticity amplitude} \\ &= \nu_t \times \langle\langle SVA \rangle\rangle; \end{aligned} \quad (8)$$

with

$$\nu_t(K) = C_H \int_K^\infty d\theta \left(\frac{E_u(\theta)}{\theta^3} \right)^{1/2},$$

where $\nu_t(K)$ is the Heisenberg's (1948) turbulent viscosity (Launder and Spalding, 1972, pp. 9–22; Pope, 1975; Staniscic, 1984, pp. 23–28; Smagorinski, 1993; Frisch, 1995, pp. 222–226 for a historical overview), $\langle\langle SVA \rangle\rangle$ is the total squared vorticity amplitude for all wavenumbers smaller than K , $\langle\langle \rangle\rangle$ is averaging over wavenumbers smaller than K , and C_H is the Heisenberg constant. Heisenberg's (1948) turbulent viscosity analogy states that the effect of eddies with wavenumbers larger than K , by which energy is withdrawn from the eddies with wavenumbers less than K , occurs as if a certain turbulent viscosity ν_t were present. The use of ν_t does not imply loss of energy from the velocity spectrum but simply a net extraction of energy from large (loss) to small (gain) eddies. Batchelor (1953, pp. 128–129) pointed out that the introduction of a turbulent viscosity to account for the energy transfer from large to small eddies can only be correct if the small eddies responsible for

the existence of such viscosity are statistically independent from the larger eddies. Katul et al. (1994a,b, 1995a,b, 1997), Praskovsky et al. (1993), and Kuznetsov et al. (1992) showed that some interaction does occur between these two types of eddy motions even at scales as small as $z/2$ for many ASL and laboratory flow types; hence, Heisenberg's (1948) model is only approximate and can only be used in a first-order analysis (see also Stanisc, 1985, pp. 193–196 and Kraichnan, 1976 for further discussion on the limitations of turbulent viscosity approaches). In order to utilize (8), a model between $\langle\langle\text{SVA}\rangle\rangle$ and E_u is required and is discussed next.

The fluctuating vorticity, defined about a given mean flow vorticity (Ω_i) is

$$\omega_i = \epsilon_{ijk} \frac{\partial u_k}{\partial x_j}$$

where ϵ_{ijk} is the alternating tensor. Tchen (1953) proposed that the SVA in (8) should be given by

$$\langle\langle\text{SVA}\rangle\rangle = \langle\langle(\omega_i\omega_i + \Omega_i\Omega_i)\rangle\rangle \quad (9)$$

when the fluctuating vorticity does not interact with the mean flow vorticity, and by

$$\langle\langle\text{SVA}\rangle\rangle = \langle\langle(\omega_i\omega_i + \omega_i\Omega_i)\rangle\rangle \quad (10)$$

when the fluctuating vorticity strongly interacts with the mean flow vorticity. Tchen's (1953) justification for (9) is that the overall amplitude of the vorticity field is strictly the independent squared sum of the mean and fluctuating vorticity for the no interaction (or no resonance) case. The coupling between the mean flow and turbulent vorticity in (10), however, insures that the mean flow vorticity field is able to create momentum exchange with eddies responsible for the generation of turbulent vorticity through the scalar product $\omega_i\Omega_i$. Such interactions in (10) occur when mean flow and turbulent vorticities have the same time scale magnitude (i.e. the mean and fluctuating vorticity are in resonance). No intermediate interaction case was considered by Tchen (1953). For these two limiting cases, S_t is given by

$$S_t = \nu_t \frac{\langle\langle\omega_i\omega_i\rangle\rangle}{P_2} + \nu_t \frac{\langle\langle\Omega_i\phi_i\rangle\rangle}{P_3} \quad (11)$$

where $\phi_i = \Omega_i$ for weak interaction, and $\phi_i = \omega_i$ for strong interaction.

Tchen (1953) showed that the functional form of P_2 and P_3 resemble the right-hand equality in (7) but with integration limits varying from zero to K rather than from zero to ∞ due to differences in the vorticity averaging operator. Hence, after adjusting integration limits for the SVA and inserting the Heisenberg viscosity model for ν_t as derived in (8) (see Hinze, 1959, p. 192; Batchelor, 1953, p. 129; Panchev, 1971, pp. 220–222 for derivation details), the spectral budget in (3) becomes:

$$\begin{aligned}
 \langle \epsilon \rangle = & 2\nu \int_0^K d\theta \theta^2 E_u(\theta) + 2B_1 \left[\int_K^\infty d\theta \left(\frac{E_u(\theta)}{\theta^3} \right)^{(1/2)} \right] \\
 & \times \left[\int_0^K d\theta \theta^2 E_u(\theta) \right] + 2B_2 \left[\int_K^\infty d\theta \left(\frac{E_u(\theta)}{\theta^3} \right)^{(1/2)} \Omega^2 \Phi(\theta) \right] \quad (12)
 \end{aligned}$$

where:

$$\begin{aligned}
 \Phi(\theta) = & \quad 1 \quad \text{weak interaction} \\
 & \frac{B_3}{B_2} \left[\frac{2 \left(\int_0^K d\theta \theta^2 E_u(\theta) \right)}{\Omega^2} \right]^{1/2} \quad \text{strong interaction} \quad (13)
 \end{aligned}$$

and B_1 , B_2 , and B_3 are constants (see Tchen, 1953, 1954; Hinze, 1959, p. 192; Panchev, 1971, p. 220), which are determined next. Also $\Omega (= (\Omega_i \Omega_i)^{1/2})$ is the magnitude of the mean vorticity. The integration limits from K to ∞ are due to ν_t being a turbulent viscosity generated from wavenumbers larger than K acting only on wavenumbers smaller than K (i.e., zero to K). The three terms on the right-hand side of (12) correspond to P_1 , P_2 , and P_3 . Hereafter, the energy balance in (12) is referred to as T53 as derived by Tchen (1953). In addition to the Heisenberg viscosity model, several other viscosity models have been proposed and reviewed in Panchev (1971, pp. 202–205). Panchev (1971, p. 202) showed that any turbulent viscosity model must satisfy several algebraic constraints and that the only model that meets such constraints is the Heisenberg model. Additional details on the derivation of (12) can be found in Hinze (1959, pp. 256–268).

2.2. APPROXIMATE SOLUTIONS FOR E_u

In this subsection, approximate $E_u(K)$ solutions for T53 are derived. Since our objective is to investigate universal power laws at low wavenumbers, we deviate from Tchen's (1953, 1954) original analysis and Panchev's (1969, 1971, p. 222) asymptotic solutions and assume, (i) solutions to T53 (if they exist) are of the form $E_u = A K^\alpha$, and (ii) the viscous dissipation term (P_1) is small relative to ($P_2 + P_3$) at low wavenumbers (see e.g., Stull, 1988, p. 167). The latter is satisfied for wavenumbers much smaller than the Kolmogorov dissipation scale ($\eta = [\nu^3 / \langle \epsilon \rangle]^{1/4}$). The approximate solutions proposed below are much simpler than the asymptotic analysis in Panchev (1971) and provide more insight into the onset of universal power law in the E_u spectrum at low wavenumbers. With this approach, constraints on when A and α are constants independent of K can be explicitly derived.

2.2.1. Strong interaction between mean flow and fluctuating vorticity

Upon replacing $E_u = A K^\alpha$ in T53, after algebraic simplifications, we obtain

$$\langle \epsilon \rangle = \frac{4B_1}{(1-\alpha)(3-\alpha)} A^{3/2} K^{(\frac{5+3\alpha}{2})} + B_3 \Omega \left(\frac{2A\sqrt{2}}{(1-\alpha)\sqrt{(3+\alpha)}} K^{1+\alpha} \right) \quad (14)$$

with the integral

$$\int_0^K d\theta \theta^2 A \theta^\alpha = \frac{AK^{3+\alpha}}{3+\alpha} - A \lim_{K \rightarrow 0} \left(\frac{K^{3+\alpha}}{3+\alpha} \right) \quad (15)$$

restricting α to values in excess of -3 in order to ensure finite $\langle \epsilon \rangle$. Re-arranging terms,

$$\left(\frac{\langle \epsilon \rangle}{\Omega B_3} \right) = \frac{1}{\Omega B_3} \frac{4B_1}{(1-\alpha)(3-\alpha)} A^{3/2} K^{(\frac{5+3\alpha}{2})} + \frac{2A\sqrt{2}}{(1-\alpha)\sqrt{(3+\alpha)}} K^{1+\alpha} \quad (16)$$

$P_2 + P_3$

where P_2 (energy transfer) and P_3 (turbulent production) are both functions of A and K . Let R be the ratio of P_2 to P_3 ($R = P_2/P_3$) and consider the algebraic solution for α for the three conditions: (i) $R \gg 1$, (ii) $R \ll 1$, and (iii) $R \sim 1$. For $R \gg 1$, (16) simplifies to

$$\left(\frac{\langle \epsilon \rangle}{\Omega B_3} \right) = \frac{1}{\Omega B_3} \frac{4B_1}{(1-\alpha)(3-\alpha)} A^{3/2} K^{(\frac{5+3\alpha}{2})} \quad (17)$$

and, since $\langle \epsilon \rangle$ and Ω on the left-hand side (LHS) of (17) are constants independent of K , the right-hand side (RHS) of (17) should be independent of K . Hence, α must be $-5/3$ to cancel the RHS dependence on K . Using $\alpha = -5/3$, $A = (\langle \epsilon \rangle / (4B_1))^{2/3}$, (17) reduces to

$$E_u = \left(\frac{1}{4B_1} \right)^{2/3} \langle \epsilon \rangle^{2/3} K^{-5/3} \quad (18)$$

which is identical to the Kolmogorov (1941) spectrum with $(4B_1)^{-2/3}$ being the Kolmogorov constant C_k . With a $C_k = 0.55$ (Kaimal and Finnigan, 1994, p. 64), $B_1 = 0.5$. The $B_1 = 0.5$ value is in excellent agreement with Proudman (1951) who reported $B_1 = 0.45 \pm 0.05$ (for a review, see Stanisc, 1985, p. 194 and Smagorinsky, 1993, Table I). Notice in (16) that $R \gg 1$ can occur if the magnitude of the mean flow vorticity (Ω) is small. Hence, the proposed T53 solution demonstrates that a $-5/3$ power law can exist at low wavenumber if the

mean flow vorticity is sufficiently small. This may explain why a $-5/3$ power law for E_u is typically observed in ASL for $Kz < 1$ despite clear violations of local isotropy assumptions (see e.g., Kaimal et al., 1972; Katul et al., 1997).

For $R \ll 1$, only the production function is relevant in (16) so that

$$\left(\frac{\langle \epsilon \rangle}{\Omega B_3}\right) = \frac{2A\sqrt{2}}{(1-\alpha)\sqrt{(3+\alpha)}} K^{1+\alpha} \quad (19)$$

and using the wavenumber independence argument of the LHS results in $\alpha = -1$ and $A = (\langle \epsilon \rangle / (B_3 \Omega))$. Therefore, $E_u(K)$ is given by

$$E_u(K) = \frac{1}{B_3} \frac{\langle \epsilon \rangle}{\Omega} K^{-1}. \quad (20)$$

This $E_u(K)$ form is a special case of Panchev's (1969; 1971, p. 222) asymptotic solution and is identical to Tchen's (1953) original solution if the energy diffusion term is neglected relative to the energy production and transfer terms. Hereafter, the spectrum in (20) is referred to as TP due to Tchen (1953, 1954) and Panchev (1969, 1971). For $R \sim 1$, no clear constant power law exists and α must vary with K .

2.2.2. Weak Interaction Between Mean Flow and Fluctuating Vorticity

The solution to T53, after algebraic simplifications, is given by

$$\frac{\langle \epsilon \rangle}{\Omega^2} = \frac{4B_1}{(1-\alpha)(3+\alpha)\Omega^2} A^{3/2} K^{(5/2+3\alpha/2)} + \frac{2B_2\sqrt{A}}{1-\alpha} K^{\frac{(\alpha-1)}{2}} \quad (21)$$

$P_2 \qquad \qquad \qquad + \qquad \qquad \qquad P_3$

which, for $R \gg 1$, is identical to (18), while for $R \ll 1$, no solution exists since

$$\frac{\langle \epsilon \rangle}{\Omega^2} = \frac{2B_2\sqrt{A}}{1-\alpha} K^{\frac{(\alpha-1)}{2}} \quad (22)$$

requires that α be unity to attain the wavenumber independence and results in an infinite $\langle \epsilon \rangle / \Omega$.

2.3. T53, TOWNSEND'S (1961) HYPOTHESIS, AND KADER AND YAGLOM'S (1991) DIMENSIONAL ANALYSIS

As noted in the introduction, the -1 power law was also derived by Perry et al. (1987) using Townsend's hypothesis and an assumed matching region for which both inner and outer flow variables describe the u and w spectra, and by Kader and Yaglom (1991) using dimensional analysis. Townsend's (1961) hypothesis states that the turbulent eddy motion in the inner region of a boundary layer consists of

an ‘active’ part which produces the shear stress $\tau_0 (= \rho u_*^2)$, and whose statistical properties are universal functions of τ_0 and z , and an ‘inactive’ irrotational part. Outer region turbulence of the boundary layer determines the statistical properties of the ‘inactive’ part, where $u_* = -\langle uw \rangle^{1/2}$ is the friction velocity, assumed to be constant independent of height, and ρ is the mean air density (see also Hogstrom, 1990). Bradshaw (1967) evaluated Townsend’s (1961) hypothesis using surface pressure data and found it to be valid for $z/h_b < 0.2$, where h_b is the boundary-layer thickness. He attributed the inactive component partly to the irrotational motion due to pressure fluctuations produced in the outer region, and partly due to the large-scale vorticity field of the outer region turbulence which the inner region senses as variability in the mean flow. Bradshaw’s analysis suggests that Townsend’s (1961) hypothesis implicitly requires that the mean flow vorticity be strongly coupled with the fluctuating vorticity field for the inner region. Based on Townsends (1961) hypothesis, Perry and Abell (1975, 1977), and Perry et al. (1986) found that the outer region scales with u_* and h_b while the inner region scales with u_* and z (see also Raupach et al., 1991). These length scales are implicit in the Kader and Yaglom (1991) dimensional analysis.

In order to derive the power spectra for the large-scale velocity perturbations and to be consistent with Kader and Yaglom’s (1990, 1991) dimensional analysis, consider the E_u spectrum normalized by the DSL characteristic length (z) and velocity (u_*) scales so that

$$\frac{E_u(K)}{u_*^2 z} = \phi_u(Kz) \quad (23)$$

where $\phi_u(Kz)$ is a similarity function (see also Monin and Yaglom, 1971). For the large-scale eddy motion restricted to $Kz \ll 1$ and $Kh_b \gg 1$, E_u should only scale with the outer-region rather than the inner-region variables as in Townsend’s (1961) hypothesis and should therefore represent the inactive eddy motion (dimensions on the order of h_b) contributing to the dynamic sublayer. Hence, E_u for the inactive eddy motion ($Kz \ll 1$) must be independent of z (Kader and Yaglom, 1991; Raupach et al., 1991; Antonia and Raupach, 1993; Katul et al., 1995a, 1996a). The height independence of the power spectrum can only be achieved if

$$\phi_u = \frac{C_{uu}}{Kz} \quad (24)$$

where $C_{uu} (\approx 0.8 - 1.1)$ is a similarity constant (Kader and Yaglom, 1984, 1991; Turan et al., 1987; Katul et al., 1995a, 1996a). This leads to a -1 power law expression for $E_u(K)$

$$E_u(K) = C_{uu} u_*^2 K^{-1} \quad (25)$$

and was originally derived and verified by Kader and Yaglom (1984, 1991) (hereafter this spectrum is referred to as KY). Turan et al. (1987) noted that C_{uu}

is sensitive to adverse pressure gradients (they reported a value of 17 for large mean adverse pressure gradients in rough pipe flows). We also note that a similar expression for $E_w (= C_{ww} u_* K^{-1})$ was derived by Kader and Yaglom (1991) with $C_{ww} = 0.35$.

The E_u expressions in (20) and (25) appear not to be identical though they both suggest an $E_u \sim K^{-1}$. We consider next whether KY is related to TP. Starting with the mean vorticity definition,

$$\Omega_i = \epsilon_{ijk} \frac{\partial \langle U_k \rangle}{\partial x_j} \quad (26)$$

the only non-zero term in a horizontally homogeneous DSL in the absence of subsidence ($\langle U_3 \rangle = 0$) is

$$\Omega_2 \approx \frac{\partial \langle U \rangle}{\partial z} = \frac{u_*}{kz} \quad (27)$$

where $k (= 0.4)$ is Von Karman's constant. Hereafter, Ω_2 is referred to as Ω for simplicity. Also, for the same assumptions, $\langle \epsilon \rangle$ is given by (see Hsieh et al., 1996; Hsieh and Katul, 1997 for discussion as to when the flux divergence term can be neglected)

$$\langle \epsilon \rangle = \langle uw \rangle \frac{\partial \langle U \rangle}{\partial z} \approx \frac{u_*^3}{kz}. \quad (28)$$

Upon replacing (27) and (28) in (20), (25) is recovered with $C_{uu} = B_3^{-1}$ so that $B_3 = 1$ for $C_{uu} = 1$. Notice that KY is only consistent with TP for strongly interacting mean-flow fluctuating vorticity. With the DSL estimates for $\langle \epsilon \rangle$ and Ω , the height-independence of the spectrum at production wavenumbers is automatically satisfied for TP.

The analysis in Tchen (1953) was restricted to homogeneous shear flows in the absence of a boundary. Tchen (1954) remarked that for a boundary-layer flow, one component of the mean flow with gradient plays a predominant role. Therefore, among energy equations for three components, one component only contains the production function giving rise to the -1 power law in E_u . These assumptions led Perry et al. (1987) to conclude that Tchen's (1953, 1954) results cannot be correct for wall-bounded shear flows since a -1 power law was also observed in their measured E_v . We should note that it is not a trivial matter to compare the predictions from Tchen's (1953, 1954) budget with one-dimensional spectra. As discussed in Panchev (1971, p. 220), the Tchen (1953, 1954) predictions are averaged over wavenumbers in all three directions in the wave vector space. Since the turbulence is anisotropic at low wavenumber, it is unclear how the wavenumber averaging modifies the E_v and E_w spectra for a three-dimensional wavenumber vector. Also, in virtually all experiments, the application of Taylor's (1938) frozen

turbulence hypothesis to terms P_2 and P_3 results in a turbulent viscosity acting only along the longitudinal wavenumber space. Extending Tchen's (1953, 1954) arguments to other velocity components requires the measurement of the full three dimensional wavenumber spectrum, and hence, the velocity field at all points in the flow domain. Tchen (1954) noted that the power laws are likely to be conserved in the transformation between the longitudinal and the three-dimensional power spectra. This conservation of power laws between one- and three-dimensional spectra is valid for the inertial range (as in K41) but has not been rigorously proven for the production range (Monin and Yaglom, 1975, pp. 355–358).

2.4. THE ONSET OF -1 AND $-5/3$ POWER-LAWS AT LOW WAVENUMBERS IN THE ATMOSPHERIC BOUNDARY LAYER (ABL)

Tchen (1953) speculated that $E_u \sim K^{-1}$ is likely to occur close to the boundary since the mechanical production of TKE is large (spectrum is dominated by P_3), while $E_u \sim K^{-5/3}$ as in (18) is likely to occur far away from the boundary when the mean flow vorticity is weakly interacting with the fluctuating vorticity. This statement may be qualitatively verified by considering the turbulent velocity perturbation equations for a neutral atmospheric boundary layer (ABL)

$$\frac{\partial u_i}{\partial t} + \frac{\partial u_i \langle U_j \rangle}{\partial x_j} + \frac{\partial \langle U_i \rangle u_j}{\partial x_j} = \nu \frac{\partial^2 u_i}{\partial x_j \partial x_j} - \frac{\partial (u_i u_j - \langle u_i u_j \rangle + \frac{p}{\rho} \delta_{ij})}{\partial x_j}. \quad (29)$$

The origin of the interaction mechanisms between the mean flow and the fluctuating vorticities is governed by terms $\partial u_i \langle U_j \rangle / \partial x_j$ and $\partial u_j \langle U_i \rangle / \partial x_j$ (see Tchen, 1953; Tennekes and Lumley, 1972, pp. 76–87). Using Townsend's (1961) hypothesis and the Perry et al. (1987) inner/outer flow length scale argument, the scale for $\partial u_i \langle U_j \rangle / \partial x_j$ and $\partial u_j \langle U_i \rangle / \partial x_j$ is of order z in the ASL and of order $h_b \gg z$ in the mixed layer (ML). The magnitude of these gradients is much smaller in the ML when compared to the ASL. Therefore, the interaction between the mean flow vorticity and the fluctuating vorticity is weak in the ML but strong in the ASL in agreement with Tchen's (1953) postulate as to why the -1 power law is not observed when z/h_b is of order unity and is also in agreement with Klebanoff's (1954) boundary-layer measurements (see Table I). The measurements in Klebanoff (1954) clearly show a -1 power law for low wavenumbers at $z/h_b = 0.05$ but not at $z/h_b = 0.8$. Even in the near-neutral ASL, a -1 power law may not be observed if the measurements are performed at a large enough z since Ω decreases linearly with z . As evidenced by (14), a small Ω reduces the contribution of the production term (P_3) relative to the transfer term (P_2).

An idealized spectrum for the DSL using approximate solutions to T53 is shown in Figure 1. The -7 power law in the far dissipation range was derived by Heisenberg (1948) and Tchen (1953) and is not considered in this study. We only note that experimental findings demonstrated that this power law is not valid

Asymptotic Solutions to T53 Budget

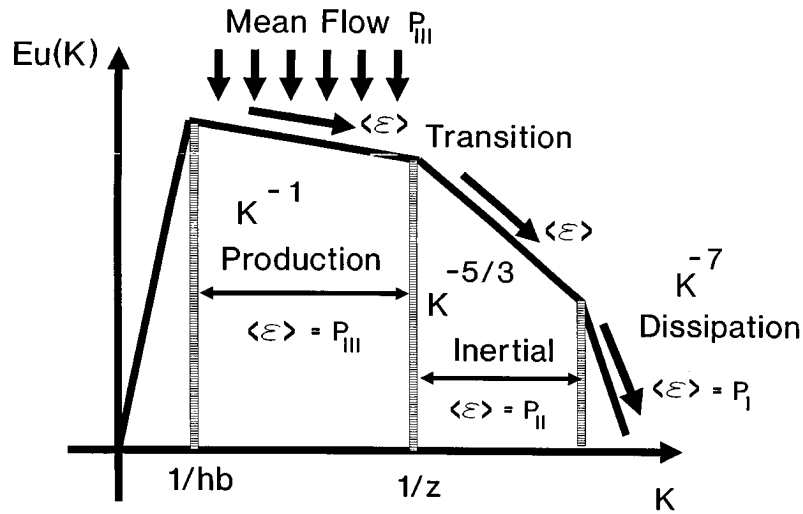


Figure 1. Expected power-laws from asymptotic solutions to T53 for the production, inertial, and viscous dissipation ranges of the u component. The solution at production scales is for strong interaction between the mean flow and turbulent vorticities.

(see e.g., Staniscic, 1985, p. 196; McComb, 1990, p. 77 for a discussion as to why Heisenberg's viscosity model fails in this range).

3. Experimental Setup

In order to investigate the low wavenumber spectral properties of the turbulent velocity in the dynamic sublayer, atmospheric surface-layer velocity measurements from three different sites along with the laboratory open channel experiment are used.

3.1. ATMOSPHERIC SURFACE-LAYER MEASUREMENTS

Table II summarizes the site characteristics and the setup at each site. The Beaufort site is a large, flat short grass farm (Open Grounds Farm) near the North Carolina coast, while the Bondville site is a large corn field ($>2 \text{ km}^2$) operated by the Illinois State Water Department Survey. The three velocity components (U_i) and temperature fluctuations (T) were measured by an Applied Technology Inc. (ATI) triaxial sonic anemometer positioned at 5 m from an estimated zero-plane displacement (see Table II). The ATI sonic path length ($= d_{sl}$) is 15 cm, the sampling duration and frequency (f_s) for these runs were 30 minutes and 10 Hz, respectively,

resulting in 18000 data points per flow variable per run. Further details about the experimental setup can be found in Katul et al. (1996b). Site 3 is a dry lakebed (Owens Lake) characterized by a heaved smooth sandy soil extending uniformly some 11 km in the north-south direction and 4 km in the east-west direction in Owens valley, California ($>44 \text{ Km}^2$). The three velocity components were measured by a Gill triaxial sonic anemometer positioned at 2.0 m–3.5 m above the ground surface. The sampling frequency and duration were 15 minutes and 56 Hz, respectively (see Katul, 1994; Katul et al., 1994a,b,c, 1995a). The runs at each site were screened and excluded if:

1. The stability parameter determined by $|z/L_{\text{mo}}| > 0.1$, where L_{mo} is the Obukhov length

$$L_{\text{mo}} = -\frac{u_*^3}{kg \frac{\langle wT \rangle}{T_a}}, \quad (30)$$

T is the turbulent temperature perturbation about the mean air temperature T_a , and $g (= 9.81 \text{ m s}^{-2})$ is the gravitational acceleration.

2. The rotation angle to bring $\langle W \rangle = 0$ was greater than 5° .

3. The wind direction standard deviation was greater than 20° .

This screening resulted in 27 runs at the Beaufort short grass site, 15 runs at the Bondville corn site, and 5 runs at Owens Lake. The number of near-neutral runs from the Owens Lake experiment was small due to the large sensible heat flux (H) and small u_* during the summer months.

3.2. OPEN CHANNEL MEASUREMENTS

The laboratory measurements were conducted at Cornell University in a 20 m long, 1.0 m wide, and 0.8 m deep open channel tilting flume with a smooth stainless steel bed. The channel slope (S_0) was set at 0.0001 resulting in a 10.3 cm ($= h_b$) water depth. The velocity was measured using a two-dimensional split-film boundary-layer probe (TSI 1287W model) that has two platinum films (1.3 mm length) coated on the top and bottom of a 0.153 mm diameter cylindrical fiber. The probe was operated with a dual-channel constant temperature anemometer (TSI 1750 model). The sampling frequency and period were 100 Hz and 81.92 seconds resulting in 8192 data points per flow variable per depth. The measurements were performed at $z = 0.1 \text{ cm}$, 0.2 cm , 0.3 cm , 0.4 cm , 0.6 cm , and 1 cm from the channel bottom. The turbulent stresses were found to be independent of height from $z = 0.6 \text{ cm}$ to $z = 1 \text{ cm}$. The friction velocity was determined from: (i) a regression fit to the logarithmic velocity profile (with $k = 0.4$) resulting in a $u_* = 0.92 \text{ cm s}^{-1}$, and (ii) $u_* = (gR_h S_0)^{1/2}$, where R_h is the hydraulic radius ($= 0.0854 \text{ m}$) resulting in $u_* = 0.89 \text{ cm s}^{-1}$. The difference between these two methods did not exceed 4% in agreement with Nezu and Rodi's (1986) experiment. Based on their recommendation as to the preferred u_* estimation method, $u_* = 0.92 \text{ cm s}^{-1}$ is

Table II
 Summary of site characteristics and location. The estimated zero-plane displacement (d) and momentum roughness height (z_0) from near-neutral runs are also shown

| Description | Site 1 | Site 2 | Site 3 |
|--------------------------------|----------------------------|-----------------------|-------------------------|
| Location | Beaufort, North Carolina | Bondville, Illinois | Owens Lake, California |
| Latitude/Longitude | 34.91°N/76.59°W | 40.05°N/88.37°W | 36.50°N/117.75°W |
| Experiment duration | August 10–October 15, 1994 | June 15–July 30, 1994 | June 20–July 2, 1993 |
| Anemometer type | ATI 3-axis sonic | ATI 3-axis sonic | Gill 3-axis sonic |
| Sampling frequency | 10 Hz | 10 Hz | 56 Hz |
| Sampling period (per run) | 27.6 min | 27.6 min | 15 min |
| Number of near-neutral runs | 27 | 15 | 5 |
| Surface Cover | Short grass | Tall Corn | Desert-like smooth sand |
| Canopy Height (m) | 0.1 | 2.4 | **** |
| Estimated z_0 (cm) | 5 | 30 | 0.014 |
| Estimated d (m) | 0 | 1.3 m | 0 |
| Measurement height ($z - d$) | 5 m | 5 m | 2.0–3.5 m |
| Estimated fetch | >1 km | >1 km | >4 km |

used. Further details about the open channel measurement setup can be found in Chu (1993).

4. Results and Discussion

In this section, the measured spectra and validation of the -1 power law are first presented. Also, we investigate the (i) upper and lower wavenumber limits for the -1 power law using T53, the dimensional analysis by KY, and Antonia and Raupach's (1993) speculations, (ii) conditions for which the mean flow and fluctuating vorticities strongly interact as proposed by Panchev (1971), and (iii) potential occurrence of a -1 power law in the vertical velocity in relation to the analysis by KY, T53, and Perry et al. (1987).

4.1. SPECTRA MEASUREMENTS AND VALIDATION OF THE -1 POWER LAW

Accurate Fourier energy spectra measurements at low wavenumbers in the ASL are limited by short sampling durations, and the need to condition measurements (i.e., windowing, tapering, etc.). The limited sampling duration prevents fragmenting the time series into many windows and typically leads to large uncertainty in the computed energy spectrum at low wavenumbers. Longer sampling durations are not possible due to potential unsteadiness in mean meteorological conditions. Conditioning the measurements may also produce undesirable distortions at low wavenumbers as discussed in Kaimal and Finnigan (1994, pp. 264–266) and Shumway (1988, pp. 68–71).

Given the uncertainty in the ASL Fourier spectra at low wavenumbers, validation of the -1 power law was carried out using the Haar wavelet spectral approach described in Katul and Parlange (1994, 1995a,b) and Katul et al. (1994 a,b). In contrast to the classical Fourier power spectrum estimation, the Haar wavelet spectral approach utilizes the full time series without any conditioning (e.g., windowing, tapering, etc.). Also, energy at wavenumbers much smaller than their Fourier counterparts can be adequately resolved, which is a key advantage for this study. The Haar wavelet basis was chosen because (i) of its short support which eliminates any edge effects that contaminate low frequency wavelet coefficients (e.g., Katul and Parlange, 1994), (ii) the differencing property of the Haar function reduces mild non-linear trend distortions at low wavenumbers, and (iii) it is frequently used in turbulence research (see e.g., Mahrt, 1991; Katul et al., 1994a,b; Katul and Vidakovic, 1996; Yee et al., 1996). For completeness, the wavelet decomposition algorithm is reviewed in the Appendix and a sample comparison between Fourier and Haar wavelet spectra is shown in Figure 2 for the open channel measurements at $z/h_b = 0.1$. The Fourier power spectrum in Figure 2 was computed by square windowing 2048 data points, de-trending the measurements within each window, cosine tapering 5% along each window edge, computing the power spectrum for

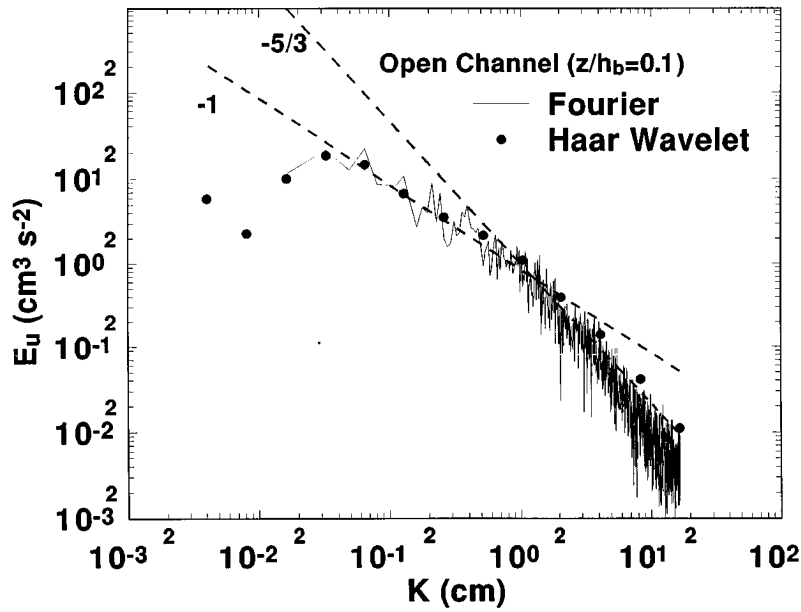


Figure 2. Comparison between Haar (solid circles) and Fourier power spectra (solid lines) for the open channel measurements at $z/h_b = 0.1$. The -1 and $-5/3$ power laws (dotted lines) are also shown.

each window, and ensemble averaging the resultant 4 spectra for each wavenumber. Notice in Figure 2 that the Haar wavelet spectrum is smoother than its Fourier counterpart and clearly reveals a -1 power law at low wavenumbers. Limitations of the Haar wavelet decomposition to resolving precise frequencies are discussed in Katul (1993).

The dimensionless Haar-wavelet longitudinal velocity spectrum ($E_u/(u_*^2 z)$) as a function of the dimensionless longitudinal wavenumber (Kz) are displayed in Figures 3a to 3c for sites 1 to 3, and in Figure 3d for the open channel measurements within the constant stress layer, respectively. Taylor's (1938) frozen turbulence hypothesis was used to convert the time to wavenumber domain. The squared turbulent intensity for all runs ($I_u^2 = [\sigma_u/\langle U \rangle]^2$) at all sites did not exceed 0.18 so that distortions resulting from the substitution of the true convection velocity by the mean longitudinal velocity are not large (see Lumley, 1965; Powell and Elderkin, 1974; Wyngaard and Clifford, 1977).

The laboratory measurements by Turan et al. (1987), and Antonia and Raupach (1993) show a clear -1 power law for $0.1 < Kz < 1$ while Kader and Yaglom's (1991) ASL measurements display a -1 power law for $0.01 < Kz < 1$. Our ASL measurements in Figures 3a to 3d exhibit a clear -1 power law for $0.1 < Kz < 1$ (though at sites 2 and 3, the -1 power law extends to Kz smaller than 0.1). The upper and lower wavenumber limits of the -1 power law are considered next.

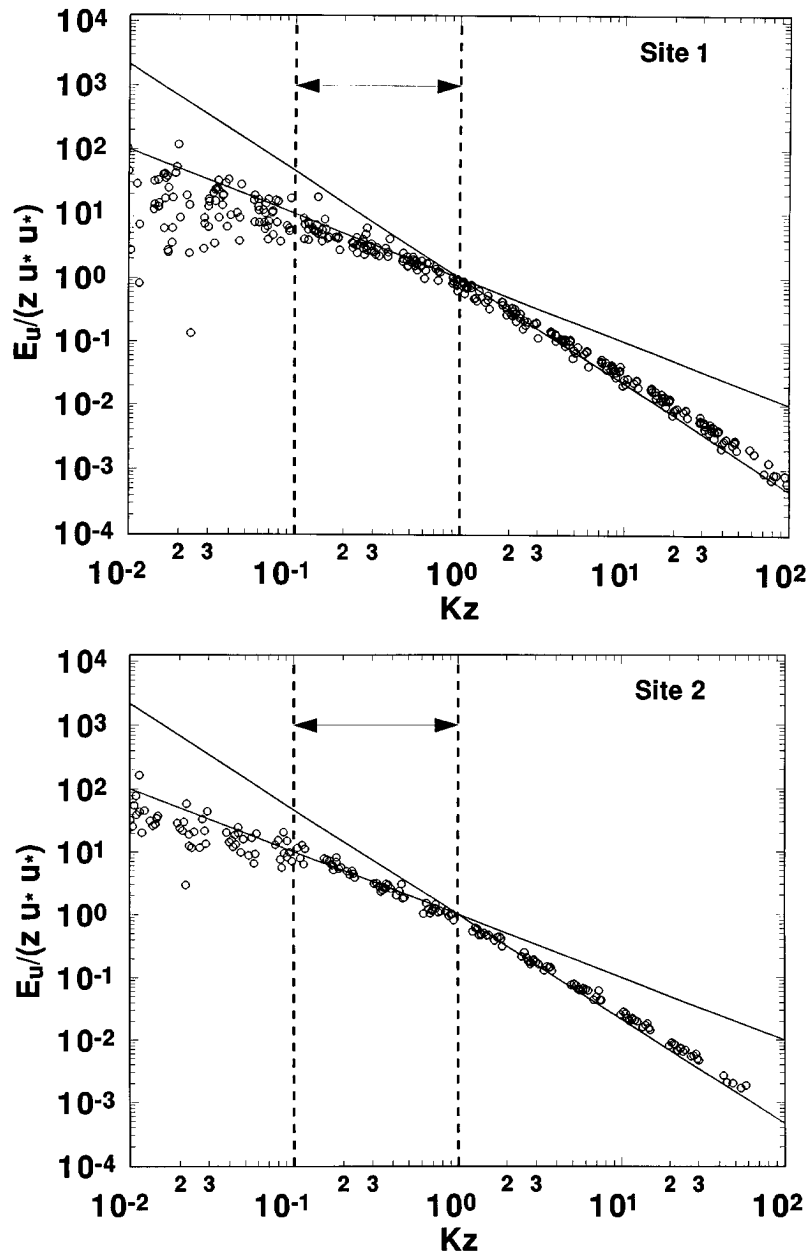


Figure 3. The relationship between the dimensionless longitudinal wavelet spectra $E_u/(z u_*^2)$ and the dimensionless wavenumber (Kz) for: (a) Site 1 (grass), (b) Site 2 (corn), (c) Site 3 (smooth sandy soil), and (d) the open channel measurements in the constant stress layer ($z/h_b = 0.04, 0.06, 0.1$). The solid line is $E_u = u_*^2 K^{-1}$. The $(Kz)^{-5/3}$ line (solid) is also shown. The dotted vertical line corresponds to the -1 power law range observed in Perry et al. (1987) when inner-flow variable scaling (z, u_*) is used.

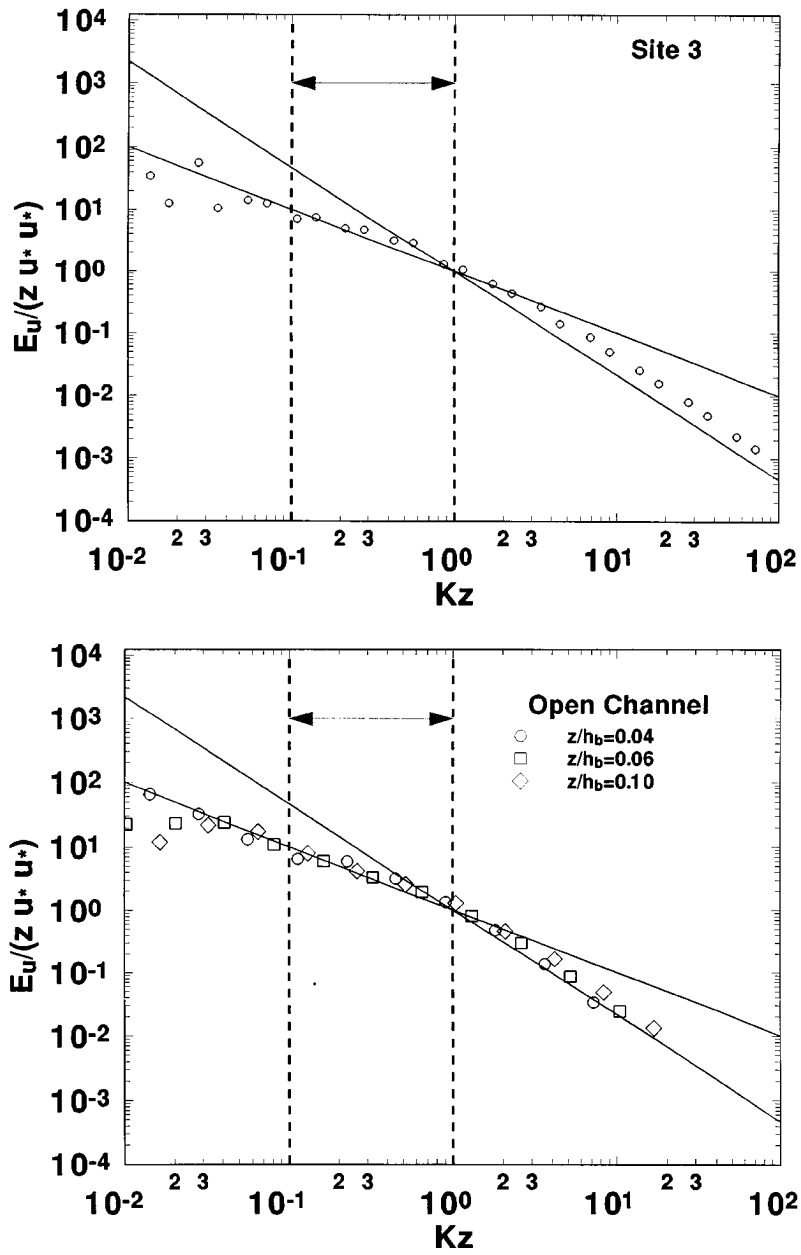


Figure 3. (Continued).

4.2. TRANSITION RANGE FROM PRODUCTION TO INERTIAL SCALES: UPPER WAVENUMBER LIMIT FOR THE -1 POWER LAW

All of the above experiments display a rapid transition from the -1 to the $-5/3$ power law, especially in the laboratory measurements of Perry et al. (1987) and

ASL measurements in Kader and Yaglom (1991). Therefore, the upper Kz limit for the -1 power law can be determined from an asymptotic matching between the production and inertial scales so that

$$C_{uu}u_*^2K^{-1} = C_K\langle\epsilon\rangle^{2/3}K^{-5/3} \Rightarrow Kz = \frac{1}{k} \left(\frac{C_K}{C_{uu}} \right)^{3/2} \quad (31)$$

(see Figure 1). Hence, with $k = 0.4$, $C_k = 0.55$, and $C_{uu} = 1.0$, the computed Kz from this matching is 1.02, which is in excellent agreement with the reported $Kz = 1$ from Perry et al. (1987), Kader and Yaglom (1991), Antonia and Raupach (1993), Katul et al. (1995a, 1996a), and the measured wavelet spectra in Figure 4 (for clarity purposes, only two decades are shown). The result in (31) was further tested in Figure 5 using the laboratory measured E_u from $z/h_b = 0.01-0.1$. Notice in Figure 5 that when no inertial subrange exists (e.g., at $z/h_b = 0.01, 0.02$), the -1 power law extends to $0.4 Kz$. As z/h_b increases, an inertial subrange emerges and the onset of the -1 power law is shifted to scales comparable to $Kz = 1$ in agreement with the predictions from (31). The above limit was derived by assuming the transition region is strictly a point (i.e., continuous but not smooth). As additional verification of this limit, (16) was differentiated twice and set to zero in order to compute the wavenumber at which maximum inflection occurs. This approach assumes that the transition region is continuous and smooth (i.e., twice differentiable). After some algebra, a non-trivial solution was derived and is given by

$$K = \frac{-2\sqrt{2}\alpha\sqrt{3+\alpha}B_3\Omega\left(\frac{2}{3+\alpha}\right)}{\sqrt{A}(15+9\alpha)B_1} \quad (32)$$

and with $\Omega = u_*/kz$, $\langle\epsilon\rangle = u_*^3/kz$, $B_1 = 0.5$, $B_3 = 1$, $\alpha = -1$, $A = \langle\epsilon\rangle/(B_3\Omega)$, and $k = 0.4$, Kz reduces to 3. Hence, at $Kz = 3 (>1)$, the maximum inflection point for which the transition from K^{-1} to $K^{-5/3}$ occurs. It should be noted that this estimate is larger than unity since the -1 power-law spectrum parameters were used in (32).

4.3. COMMENT ON KY AND TP SPECTRA NEAR THE TRANSITION REGION

It is important to note that the extension of the -1 power law to scales comparable to $Kz = 1$ (transition region) cannot be consistent with the key assumption of KY, namely that $Kz \ll 1$. Since (20) and (25) are, in fact identical, we consider whether (20) also suffers from the same limitation. As shown in (16), the -1 power law can only be derived if $R \ll 1$. Given the estimates of A , B_1 , and Ω , it is possible to check whether R is small at $Kz = 1$. Based on our proposed definition of R and after some algebra, R simplifies to

$$R = \frac{B_1\sqrt{2}A^{1/2}}{\sqrt{(3+\alpha)\Omega}}K^{\frac{\alpha+3}{2}} \quad (33)$$

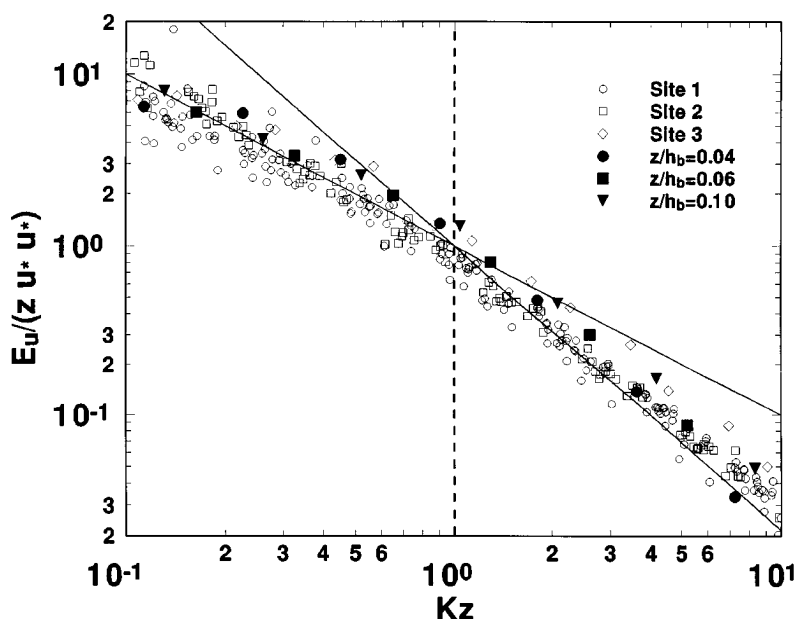


Figure 4. The transition from production to inertial (K41) scales. The dotted vertical line is the wavenumber computed by matching K41 ($-5/3$ power law) and TP (-1 power law) spectra. The solid lines $(Kz)^{-1}$ and $(Kz)^{-5/3}$ are also shown.

and with $\alpha = -1$, $A = \langle \epsilon \rangle / (B_3 \Omega)$, $\langle \epsilon \rangle = u_*^3 / kz$, $\Omega = u_* / kz$, $B_1 = 0.5$, and $B_3 = 1$, $R \sim 0.2(Kz)$. Therefore, at $Kz = 1$, $R = 0.2$ suggesting that P_3 (production) is an order of magnitude larger than P_2 (transfer). Hence, the fact that laboratory (see e.g., review in Raupach et al., 1991) and ASL (Kader and Yaglom, 1991; Katul et al., 1995a, 1996a) measurements exhibit a -1 power law up to $Kz = 1$ followed by a $-5/3$ power law is consistent with (20) but not with the height-independence argument of (25).

4.4. MEAN AND TURBULENT FLOW VORTICITY INTERACTION: A LOWER WAVENUMBER LIMIT FOR THE -1 POWER LAW

Thus far, practical methods to *a priori* estimate whether the mean flow and the turbulent vorticity are strongly interacting have not been well developed, with the exception of the comment in Panchev (1971, p. 220) and the argument in Claussen (1985), which follows from the assumption of Panchev (1971). In Panchev (1971, p. 220), the interaction between the mean and fluctuating vorticity is considered

$$\begin{aligned}
 \text{weak if } \frac{\partial \langle U \rangle}{\partial z} &\ll \sqrt{\langle \text{curl} u_i^2 \rangle} = \left(\frac{\nu}{\langle \epsilon \rangle} \right)^{-1/2} \\
 \text{strong if } \frac{\partial \langle U \rangle}{\partial z} &\approx \left(\frac{\nu}{\langle \epsilon \rangle} \right)^{-1/2}.
 \end{aligned} \tag{34}$$

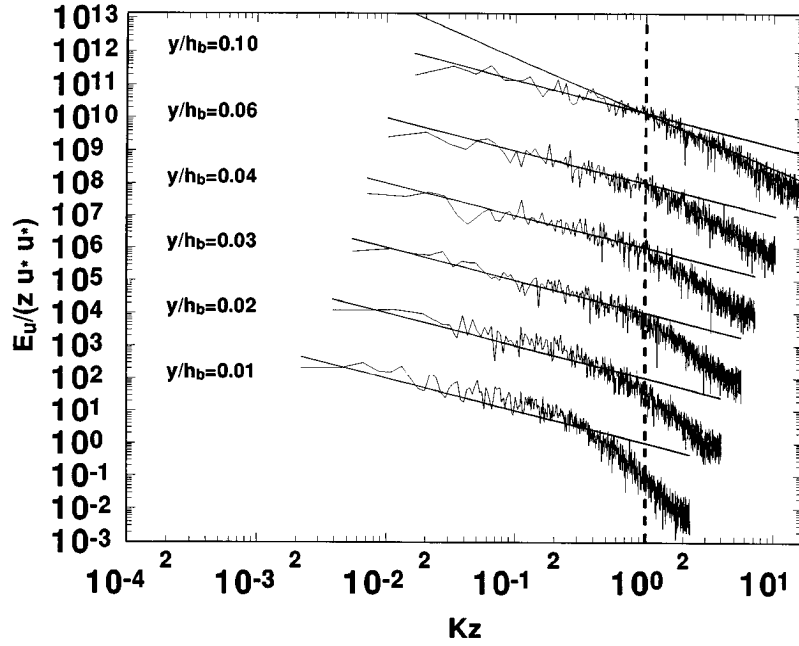


Figure 5. The relationship between the dimensionless longitudinal velocity Fourier spectra $E_u/(zu_*^2)$ and the dimensionless wavenumber (Kz) for the open channel measurements for $z/h_b = 0.01, 0.02, 0.03, 0.04, 0.06$ and 0.1 . The spectra are shifted upward by two decades to permit comparisons between different transition regions neighboring $Kz = 1$. The solid line is $E_u = u_*^2 K^{-1}$ and the dotted line is $Kz = 1.0$.

Here, the Kolmogorov time scale is used as a measure of the fluctuating vorticity time scale. We show that such an estimate cannot be correct in the DSL and investigate a new criterion for establishing whether the mean flow and fluctuating vorticity are strongly interacting.

Using $\langle \epsilon \rangle = u_*^3/kz$ and $\partial \langle U \rangle / \partial z = u_*/kz$ in (34), the criterion by Panchev (1971) can be reformulated using a Reynolds number $Re (= kz u_*/\nu)$ such that Re must be of order unity for the mean and turbulent vorticity to be strongly interacting. In the DSL, $Re \sim 10\,000 \gg 1$ suggesting that a -1 power law cannot exist. This criterion is in direct conflict with the measurements of Kader and Yaglom (1991), Katul et al. (1995a, 1996a) and the present DSL experiment (Figures 3a to 3d).

In the derivation of terms P_2 and P_3 , the turbulent vorticity at low wavenumbers is of order

$$\langle \langle \omega_i \omega_i \rangle \rangle \sim 2 \int_0^K d\theta \theta^2 E_u(\theta) \sim 2 \int_0^K d\theta \theta^2 C_{uu} u_*^2 \theta^{-1} \approx K^2 u_*^2. \quad (35)$$

In (35), it is assumed that the mean and fluctuating vorticity are interacting (or in resonance). The ratio of turbulent to mean-flow vorticity magnitudes ($V_R = K u_*/\Omega$) becomes $K u_*/(u_*/kz) = 0.4 K z$. For resonance to occur between the

mean and fluctuating vorticities, $V_R (= 0.4Kz)$ must be of order unity. A direct consequence of such an order of magnitude argument is that maximum interaction between mean and turbulent vorticities occurs at scales Kz of order $1/0.4$, which is of order unity. In addition, the interaction between the mean and fluctuating vorticity becomes weak for $K \ll z$ since $V_R \rightarrow 0$. Hence, the -1 power law can not extend to $Kz \sim 0$. It is difficult to assess the lower-wavenumber limit of the -1 power law in the ASL due to uncertainties in h_b . Nevertheless, the laboratory open channel measurements (Figure 3d) suggest that the -1 power law extends to $Kh_b \sim 1.25$. This limit is in agreement with Antonia and Raupach (1993) who speculated that the -1 power law must extend to $Kh_b = 1.2$ from wind tunnel velocity measurements. Yaglom (1994) suggested that the -1 power law should be restricted to $Kh_b \gg 1$ in the DSL which is at variance with Figure 3d and the measurements of Antonia and Raupach (1993). We note that in the ABL, eddies whose length scales are much larger than z are influenced by factors such as inhomogeneity in the static pressure field (e.g., Hogstrom, 1990), ground-heat thermal inhomogeneity (Yaglom, 1993; Kader and Yaglom, 1990), and possibly are contaminated by mesoscale disturbances (Yaglom, 1994). Hence, for ASL turbulence, the existence of a -1 power law up to scales $Kh_b \sim 1.2$ is less likely though it appears to be the case in many laboratory measurements.

Since the turbulent vorticity is difficult to measure, we cannot directly verify (35). However, our proposed criterion appears to be much more consistent with the results in Figure 4 when compared to Panchev's (1971) criterion since: (1) η is not an important factor (note: η for the two fluids in Figure 4 differed by an order of magnitude yet the -1 power for the flume and ASL were the same with identical lower and upper wavenumber limits), and (2) the -1 power law is well defined up to scales comparable to $10z$ but not larger. For $Kz \ll 0.1$, the -1 power law does not exist at site 1. We also note that this -1 power law range ($0.1 \leq Kz \leq 1$) is in excellent agreement with the overlap region between outer and inner flow scaling of Perry et al. (1987).

4.5. COMMENTS ON THE VERTICAL VELOCITY SPECTRA

The dimensionless vertical velocity spectrum ($E_w/(u_*^2 z)$) as a function of the dimensionless longitudinal wavenumber (Kz) are displayed in Figure 6a for sites 1 to 3 and the open channel measurements within the constant stress layer. The -1 power law (solid line) in Figure 6a is $E_w = 0.35u_*^2 K^{-1}$ and is the best fit power law to the DSL spectra measurements by Kader and Yaglom (1991). No clear -1 power law exists at $Kz \ll 1$ suggesting that the dimensional analysis in Kader and Yaglom (1991) is not valid for E_w . Katul and Parlange (1995a) observed a limited -1 power law in their E_w spectra but for $Kz > 1$. The absence of a -1 power law at $Kz \ll 1$ in the E_w spectrum is consistent with the inactive eddy hypothesis in Perry et al. (1987). From Perry et al. (1987), only inner-flow scaling and K41 scaling are expected for E_w . Tchen (1954) also argued against a -1 power

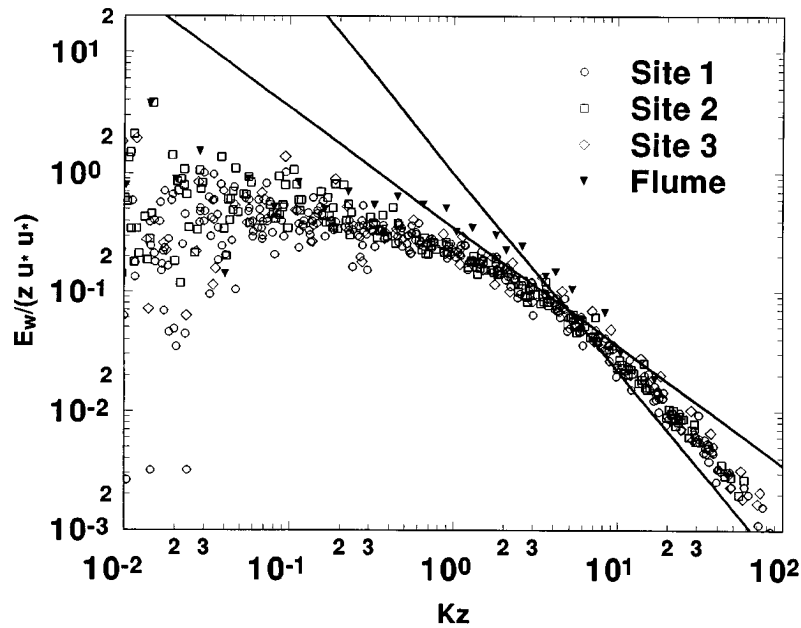


Figure 6a. Same as Figure 3 but for the dimensionless vertical velocity spectra $E_w / (z u_* u_*^2)$. The open channel flume measurements (solid triangle) are for $z/h_b = 0.04, 0.06, \text{ and } 1.0$. The -1 power law ($E_w = 0.36 u_*^2 K^{-1}$) is a best fit to the data by Kader and Yaglom (1991). The $-5/3$ power law is also shown.

law in the E_w spectrum since the production function (P_3) is absent (at least for a near-neutral ASL). For further verification of the absence of a -1 power law in the E_w spectrum, we show the Fourier spectra for the open channel experiment in Figure 6b.

5. Summary and Conclusions

The longitudinal velocity power spectrum (E_u) at low wavenumbers (K) was examined theoretically using newly derived approximate solutions to a spectral budget equation (T53) proposed by Tchen (1953) and experimentally using atmospheric surface layer and open channel measurements. This study demonstrated the following:

1. In contrast to speculations by Claussen (1985), Raupach et al. (1991), and Antonia and Raupach (1993), a -1 power law was measured and modelled in the near-neutral atmospheric surface layer. Based on T53, a necessary (but not sufficient) condition for the occurrence of a -1 power law in the E_u spectrum is the strong interaction between the mean flow and turbulent vorticities. Contrary to arguments in Panchev (1971), such interaction is possible for $0.1 \leq Kz \leq 1.0$.

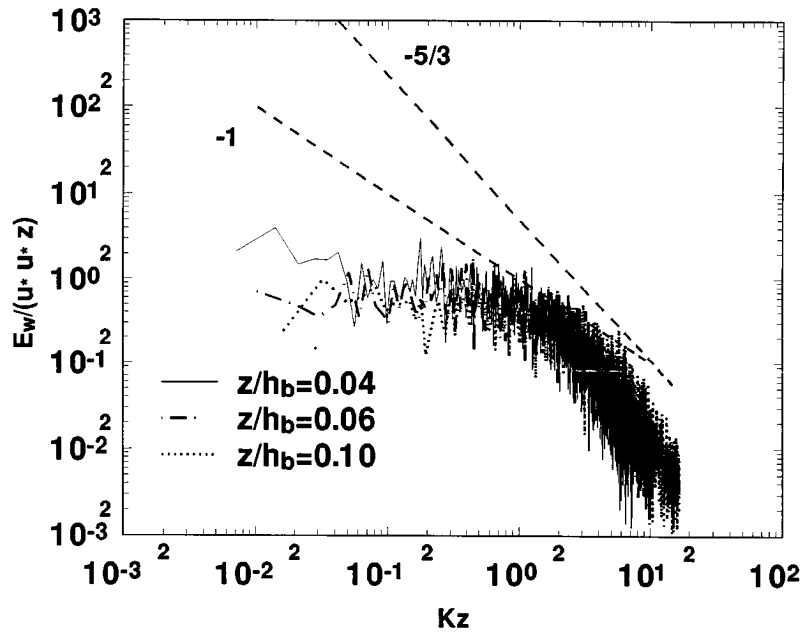


Figure 6b. The Fourier dimensionless vertical velocity spectra $E_w/(zu_*^2)$ for the open channel measurements in the constant stress layer. The -1 and $-5/3$ power laws are also shown.

2. When the velocity sampling duration is limited by steadiness in the mean meteorological conditions, orthonormal wavelet spectra are better suited than their Fourier counterpart for investigating such power-law occurrences at low-wavenumbers.

3. The two formulations resulting in $E_u \sim K^{-1}$ include: (i) $E_u = B_3^{-1}[\langle \epsilon \rangle / \langle \Omega \rangle] K^{-1}$ obtained by solving T53 (referred to as TP), where $\langle \epsilon \rangle$ and Ω are the mean turbulent kinetic energy dissipation per unit mass and the mean flow vorticity, respectively, and (ii) $E_u = C_{uu}[u_*^2] K^{-1}$ obtained from dimensional analysis for $Kz \ll 1$ (referred to as KY). It was shown that these two spectral formulations are identical in the dynamic sublayer. However, underlying assumptions in the derivation of KY and TP are not identical. The KY spectrum is derived from a height independence argument that requires $Kz \ll 1$ while the TP spectrum is derived from the relative importance of the production (P_3) to transfer functions (P_2). It was shown that the TP derivation is consistent with both laboratory and field measurements.

4. Using T53, it was demonstrated that the TP spectrum extends to $Kz \sim 1$ in agreement with laboratory and field experiments. The validity of TP at $Kz \sim 1$ was demonstrated from (i) asymptotic matching between K41 and TP, and (ii) a maximum inflection analysis. The dimensional analysis of Kader and Yaglom

(1984, 1991) assumes, a priori, that $Kz \ll 1$, and hence, no -1 power law should exist for scales comparable to z following their height-independence argument.

5. Contrary to the dimensional analysis of KY, the -1 power law was absent from the vertical velocity spectrum in the DSL for $Kz \ll 1$. This absence is consistent with the inactive eddy-hypothesis of Townsend (1976), the analysis by Perry et al. (1987), and the arguments in Tchen (1954).

6. The similarity constant $C_{uu} (\approx 1)$ from the KY spectrum was related to the Heisenberg constant B_3 and was shown to be independent of wall roughness and fluid viscosity in the dynamic sublayer. Also, the measured B_3 from this experiment is in excellent agreement with a previously reported value by Proudman (1951). This finding is contrary to the experimental findings of Krogstad et al. (1992). The fact that C_{uu} is independent of surface roughness for $Kz \leq 1$ is also in agreement with the inactive eddy hypothesis.

Acknowledgments

The authors would like to thank Peter Finkelstein, Eric Hebert, and John Clarke for their measurements at the Illinois State Water Survey Research Station in Bondville (Illinois) and at the Open Grounds Farm in Beaufort (North Carolina), Marc Parlange and John Albertson for their help and support at Owens lake (California), and Anthony Perry and the editors for their helpful comments. This project was supported, in part, by the Environmental Protection Agency (EPA) under cooperative agreement 91-0074-94 (CR817766), the National Science Foundation (NSF) through Grant BIR-9512333, and the U.S. Department of Energy (DOE) through the Southeast Regional Center at the University of Alabama, Tuscaloosa (DOE Cooperative Agreement No. DE-FC03-90ER61010), and through FACTS-I (DOE Cooperative Agreement No. DE-FG05-95 ER62083).

Appendix: Orthonormal Wavelet Expansion and Wavelet Spectra Algorithm

For discrete turbulence measurements of a flow variable $f(x)$, discrete orthonormal wavelet transforms (DWT) are preferred over continuous wavelet transforms (CWT) since the flow variable $f(x)$ is known at discrete points x_j only. Furthermore, the over-complete description of $f(x_j)$ introduces redundant information that can be injected into the wavelet transform of $f(x_j)$ and can produce artificial correlations among the wavelet coefficients. Such correlations are strictly a property of the wavelet transform and not of the turbulence phenomena under consideration. In orthonormal wavelets, the decomposition is not over-complete and basis function are orthogonal so that mutual independence amongst the wavelet coefficients is guaranteed.

As shown in Katul and Parlange (1994), the edge effects of the wavelet transform amplify at low wavenumbers with increasing wavelet support. The shortest

compactly supported wavelet is the Haar and this basis is adopted for the -1 power law investigations. Much of this material is presented in Katul and Parlange (1994), Katul et al. (1994), and Szilagyi et al. (1996), but for completeness, the key steps in the wavelet spectra calculations are shown.

The Haar basis $\psi(x) = (a^{-1/2})\psi((x - b)/a)$, where $a = 2^m$ and $b = 2^m i$ for $i, m \in Z$ (the set of integers), is given by

$$\psi(x) = \begin{cases} 1 & \text{for } 0 < x < 1/2 \\ -1 & \text{for } 1/2 \leq x < 1 \\ 0 & \text{elsewhere.} \end{cases} \quad (36)$$

For this basis function, the discrete wavelet coefficients $WT^{(m+1)}(k)$ and the coarse grained signal $S^{(m+1)}(k)$ at scale $m + 1$ can be determined from the signal $S^{(m)}$ at scale m using

$$WT^{(m+1)}(i) = \frac{1}{\sqrt{2}}[S^{(m)}(2i - 1) - S^{(m)}(2i)] \quad (37)$$

$$S^{(m+1)}(i) = \frac{1}{\sqrt{2}}[S^{(m)}(2i - 1) + S^{(m)}(2i)] \quad (38)$$

where m is a scale index that varies from 0 to $M - 1$, i is a position index that varies from 0 to $2^{M-m-1}-1$, and $M = \log_2(N)$, N is the number of samples in the time interval (integer power of 2). For the Haar wavelet, the coarse grained signal defined by (38) is a low-pass filtered function obtained by a simple block moving average, while the wavelet coefficients are computed from the high-pass filter in (37). The wavelet coefficients and coarse grained signal may be calculated by the following pyramidal algorithm:

(1) Beginning with $m = 0$, use (37) and (38) to calculate the signal $S(1)$ and the coefficients $WT(1)$ at the first scale by looping over i from 0 to $2^{M-1}-1$. This will result in S and WT vectors each of length $N/2$. The raw velocity measurements are stored in $S(0)$.

(2) Repeat step 1 with $m = 1$ to calculate the next coarser scale's pair of vectors $S^{(2)}$ and $WT^{(2)}$ (each of length $N/4$).

(3) Repeat for larger scale m up to $M - 1$ to produce a series of S and WT vectors of progressively decreasing length. Note that at $m = M - 1$ the coarse grained signal converges to a point.

This algorithm yields $N - 1$ wavelet coefficients that define the orthonormal Haar wavelet transform of the measured turbulence signal. The above pyramidal procedure, which is the basis of Fast Wavelet Transforms (FWT), requires on the order of N computations vis-a-vis the $N \log_2 N$ computations for Fast Fourier Transforms (FFT). For other wavelet bases, the algorithm in Press et al. (1992, pp. 586–590) can be used.

The set of $N - 1$ discrete Haar wavelet coefficients satisfies the conservation of energy condition

$$\sum_{j=0}^{N-1} f(j)^2 = \sum_{m=1}^M \sum_{i=0}^{2^{M-m}-1} WT^{(m)}(i). \quad (39)$$

The variance (σ^2) of the turbulence measurement, in terms of the wavelet coefficients, can be deduced from this energy conservation using

$$\sigma^2 = N^{-1} \sum_{m=1}^M \sum_{i=0}^{2^{M-m}-1} (WT^{(m)}[i])^2. \quad (40)$$

The total energy T_E contained in scale $R_m (= 2^m dy)$ can be computed from the sum of the squared wavelet coefficients at scale index (m) so that

$$T_E = N^{-1} \sum_{i=0}^{2^{M-m}-1} (WT^{(m)}[i])^2 \quad (41)$$

where $dy (= f_s^{-1} \langle U \rangle)$ is the measurement spacing in physical space (estimated from Taylor's hypothesis). In order to compare the wavelet power spectrum to the Fourier spectrum, we define a wavenumber K_m , corresponding to scale R_m as

$$K_m = \frac{2\pi}{R_m}. \quad (42)$$

Hence, the power spectral density function $E(K_m)$ is computed by dividing T_E by the change in wavenumber $\Delta K_m (= 2\pi 2^{-m} dy^{-1})$ so that

$$E(K_m) = \frac{\langle (WT^{(m)}[i])^2 \rangle dy}{2\pi} \quad (43)$$

where $\langle \langle \cdot \rangle \rangle$ is averaging in space over all values of the position index (i) at scale index (m) (see Meneveau, 1991a; Katul and Parlange, 1994). We note that Meneveau (1991), Katul and Parlange (1994), and Katul et al. (1994) used $\Delta K_m (= 2\pi 2^{-m} dy^{-1} \ln(2))$. Recently, Szilagyi et al. (1996) demonstrated that $\Delta K_m (= 2\pi 2^{-m} dy^{-1})$ is a superior approximation to dK_m . The wavelet power spectrum at wavenumber K_m is directly proportional to the average of the squared wavelet coefficients at that scale. Because the power at wavenumber K_m is determined from averaging many squared wavelet coefficients, the wavelet power spectra are smoother than their Fourier counterparts as shown in Katul and Parlange (1994, 1995), Katul et al. (1994), and Szilagyi et al. (1996).

References

- Antonia, R. A. and Raupach, M. R.: 1993, 'Spectral Scaling Laws in a High Reynolds Number Laboratory Boundary Layer', *Boundary-Layer Meteorol.* **65**, 289–306.

- Batchelor, G. K.: 1953, *The Theory of Homogeneous Turbulence*, Cambridge University Press, 197 pp.
- Bradshaw, P.: 1967, 'Inactive Motion and Pressure Fluctuations in Turbulent Boundary Layers', *J. Fluid Mech.* **30**, 241–258.
- Brutsaert, W.: 1982, *Evaporation into the Atmosphere: Theory, History, and Applications*, Kluwer Academic Publishers, 299 pp.
- Bremhorst, K. and Bullock, K. J.: 1970, 'Spectral Measurements of Temperature and Longitudinal Velocity Fluctuations in Fully Developed Pipe Flow', *Int. J. Heat Mass Transfer* **13**, 1313–1329.
- Bremhorst, K. and Walker, T. B.: 1973, 'Spectral Measurements of Turbulent Momentum Transfer in Fully Developed Pipe Flow', *J. Fluid Mech.* **61**, 173–186.
- Bullock, K. J., Cooper, R. E., and Abernathy, F. H.: 1978, 'Structural Similarity in Radial Correlations and Spectra of Longitudinal Velocity Fluctuations in Pipe Flow', *J. Fluid Mech.* **88**, 585–608.
- Canuto, V. M. and Goldman, I.: 1985, 'Analytical Model for Large-Scale Turbulence', *Phys. Rev. Lett.* **54**, 430–433.
- Chu, C. R.: 1993, *Experiments on Gas Transfer and Turbulence Structure in Free Surface Flows with Shear*, Ph.D. Dissertation, Cornell University, Ithaca, New York, 191 pp.
- Claussen, M.: 1985, 'A Model of Turbulence Spectra in the Atmospheric Surface Layer', *Boundary-Layer Meteorol.* **33**, 151–172.
- Erm, L. P., Smits, A. J., and Joubert, P. N.: 1987, 'Low Reynolds Number Turbulent Boundary Layers on a Smooth Flat Surface in a Zero Pressure Gradient', in F. Durst, B. E. Launder, J. L. Lumley, F. W. Schmidt, and J. H. Whitelaw (eds.), *Turbulent Shear Flows 5*, Springer-Verlag, Berlin, pp. 186–196.
- Erm, L. P. and Joubert, P. N.: 1991, 'Low Reynolds Number Turbulent Boundary Layers', *J. Fluid Mech.* **230**, 1–44.
- Frisch, U.: 1995, *Turbulence*, Cambridge University Press, 296 pp.
- Garratt, J. R.: 1992, *The Atmospheric Boundary Layer*, Cambridge University Press, 316 pp.
- Gorshkov, N. F.: 1967, 'Measurements of the Spectrum of Pressure Micropulsations in Near-Earth Layer of the Atmosphere', *Izv. Atmos. Oceanic Phys.* **3**, 447–451.
- Heisenberg, W.: 1948, 'Zur Statistischen Theorie der Turbulenz', *Z. Physik* **124**, 628–657.
- Hinze, J. O.: 1959, *Turbulence*, McGraw-Hill, New York, 586 pp.
- Högström, U.: 1990, 'Analysis of Turbulence in the Surface Layer with a Modified Similarity Formulation for Near Neutral Conditions', *J. Atmos. Sci.* **47**, 1949–1972.
- Hunt, I. A. and Joubert, P. N.: 1979, 'Effects of Small Streamline Curvature on Turbulent Duct Flow', *J. Fluid Mech.* **91**, 633–659.
- Hsieh, C. I., Katul, G. G., Schieldge, J., Sigmon, J., and Knoerr, K.: 1996, 'Estimation of Momentum and Heat Exchanges Using Dissipation and Flux-Variance Methods in the Unstable Surface Layer', *Water Resources Res.* **32**, 2453–2462.
- Hsieh, C. I. and Katul, G. G.: 1997, 'Dissipation Methods, Taylor's Hypothesis, and Stability Correction Functions in the Atmospheric Surface Layer', *J. Geophys. Res.* **102**, 16391–16405.
- Kader, B. A. and Yaglom, A. M.: 1984, 'Turbulent Structure of an Unstable Atmospheric Layer', in R. Z. Sagdeyev (ed.), *Nonlinear and Turbulent Processes in Physics*, vol. 2, pp. 829–845, Harwood Academic, Boston, MA.
- Kader, B. A. and Yaglom, A. M.: 1990, 'Mean Fields and Fluctuation Moments in Unstably Stratified Turbulent Boundary Layers', *J. Fluid Mech.* **212**, 637–662.
- Kader, B. A. and Yaglom, A. M.: 1991, 'Spectra and Correlation Functions of Surface Layer Turbulence in Unstable Thermal Stratification', in O. Metais and M. Lesieur (eds.), *Turbulence and Coherent Structures*, Kluwer Academic Press, Dordrecht, pp. 388–412.
- Kader, B. A.: 1992, 'Determination of Turbulent Momentum and Heat Fluxes by Spectral Methods', *Boundary-Layer Meteorol.* **61**, 323–347.
- Kaimal, J. C., Wyngaard, J. C., Izumi, Y., and Cote, O. R.: 1972, 'Spectral Characteristics of Surface Layer Turbulence', *Quart. J. Roy. Meteorol. Soc.* **98**, 563–589.
- Kaimal, J. C. and Finnigan, J. J.: 1994, *Atmospheric Boundary Layer Flows: Their Structure and Measurement*, Oxford University Press, 289 pp.

- Katul, G. G.: 1993, *Coupled Processes Near the Land-Atmosphere Interface*, Ph.D. Dissertation, Department of Civil and Environmental Engineering, University of California, Davis, California, 193 pp.
- Katul, G. G.: 1994, 'A Model for Sensible Heat Flux Probability Density Function for Near-Neutral and Slightly-Stable Atmospheric Flows', *Boundary-Layer Meteorol.* **71**, 1–20.
- Katul, G. G. and Parlange, M. B.: 1994, 'On the Active Role of Temperature in Surface Layer Turbulence', *J. Atmos. Sci.* **51**, 2181–2195.
- Katul, G. G., Parlange, M. B., and Chu, C. R.: 1994a, 'Intermittency, Local Isotropy, and Non-Gaussian Statistics in Atmospheric Surface Layer Turbulence', *Phys. Fluids* **6**, 2480–2492.
- Katul, G. G., Albertson, J. D., Chu, C. R., and Parlange, M. B.: 1994b, 'Intermittency in Atmospheric Surface Layer Turbulence: The Orthonormal Wavelet Representation', in E. Foufoula Georgiou and Praveen Kumar (eds.), *Wavelets in Geophysics*, pp. 81–105, Academic Press.
- Katul, G. G., Albertson, J. D., Parlange, M. B., Chu, C. R., and Stricker, H.: 1994c, 'Conditional Sampling, Bursting, and the Intermittent Structure of Sensible Heat Flux', *J. Geophys. Res.* **99**, 22869–22876.
- Katul, G. G. and Parlange, M. B.: 1995a, 'The Spatial Structure of Turbulence at Production Wavenumbers Using Orthonormal Wavelets', *Boundary-Layer Meteorol.* **75**, 81–108.
- Katul, G. G. and Parlange, M. B.: 1995b, 'Analysis of Land Surface Fluxes Using the Orthonormal Wavelet Transform', *Water Resources Res.* **31**, 2743–2749.
- Katul, G. G., Chu, C. R., Parlange, M. B., Albertson, J. D., and Ortenburger, T. A.: 1995a, 'The Low-Wave Number Spectral Characteristics of Turbulent Velocity and Temperature in the Unstable Atmospheric Surface Layer', *J. Geophys. Res.* **100**, 14243–14255.
- Katul, G. G., Parlange, M. B., Albertson, J. D., and Chu, C. R.: 1995b, 'Local Isotropy and Anisotropy in the Sheared and Heated Atmospheric Surface Layer', *Boundary-Layer Meteorol.* **72**, 123–148.
- Katul, G. G., Parlange, M. B., Albertson, J. D., and Chu, C. R.: 1995c, 'The Random Sweeping Decorrelation Hypothesis in Stratified Turbulent Flows', *Fluid Dynamics Research* **16**, 275–295.
- Katul, G. G. and Vidakovic, B.: 1996, 'The Partitioning of Attached and Detached Eddy Motion in the Atmospheric Surface Layer Using Lorentz Wavelet Filtering', *Boundary-Layer Meteorol.* **77**, 153–172.
- Katul, G. G., Albertson, J. D., Hsieh, C. I., Conklin, P. S., Sigmon, J. T., Parlange, M. B., and Knoerr, K. R.: 1996a, 'The Inactive Eddy-Motion and the Large-Scale Turbulent Pressure Fluctuations in the Dynamic Sublayer', *J. Atmos. Sci.* **53**, 2512–2524.
- Katul, G. G., Finkelstein, P., Clarke, J., and Ellstad, T.: 1996b, 'An Investigation of the Conditional Sampling Method Used to Estimate Fluxes of Active, Reactive, and Passive Scalars', *J. Appl. Meteorol.* **35**, 1835–1845.
- Katul, G. G., Hsieh, C. I., and Sigmon, J.: 1997, 'Energy-Inertial Scale Interactions for Velocity and Temperature in the Unstable Atmospheric Surface Layer', *Boundary-Layer Meteorol.* **82**, 49–80.
- Klebanoff, P. S.: 1954, 'Characteristics of Turbulence in a Boundary Layer with Zero-Pressure Gradient', Report 1247, *National Advisory Committee for Aeronautics*, National Bureau of Standards, Washington D.C., 1–28.
- Korotkov, B. N.: 1976, 'Some Types of Local Self-Similarity of the Velocity Field of Wall Turbulent Flows', *Izv. Akad. Nauk SSSR, Ser. Mekh. Zhidk. i. Gaza* **6**, 35–42.
- Kolmogorov, A. N.: 1941, 'The Local Structure of Turbulence in Incompressible Viscous Fluid for Very Large Reynolds Numbers', *Dokl. Akad. Nauk SSSR* **30**, 299–304.
- Kraichnan, R. H.: 1976, 'Eddy Viscosity in Two and Three Dimensions', *J. Atmos. Sci.* **33**, 1521–1536.
- Krogstad, P. A., Antonia, R. A. and Browne, W. B.: 1992, 'Comparison Between Rough and Smooth Wall Turbulent Boundary Layers', *J. Fluid Mech.* **245**, 599–617.
- Kuznetsov, V. R., Praskovskiy, A., and Sabelnikov, V. A.: 1992, 'Fine-Scale Turbulence Structure of Intermittent Shear Flows', *J. Fluid Mech.* **243**, 595–622.
- Launder, B. E. and Spalding, D. B.: 1972, *Mathematical Models of Turbulence*, Academic Press, New York, 169 pp.
- Lumley, J.: 1965, 'Interpretation of Time Spectra Measured in High Intensity Shear Flows', *Phys. Fluids* **6**, 1056–1062.
- Mahrt, L.: 1991, 'Eddy Asymmetry in the Sheared-Heated Boundary Layer', *J. Atmos. Sci.* **48**, 472–492.

- McComb, W. D.: 1990, *The Physics of Fluid Turbulence*, Oxford Science Publications, 572 pp.
- Monin, A. S. and Obukhov, A. M.: 1954, 'Basic Laws of Mixing in the Ground Layer of the Atmosphere', *Tr. Geofiz. Inst. Akad. Nauk. SSSR* **151**, 163–187.
- Monin, A. S. and Yaglom, A. M.: 1971, *Statistical Fluid Mechanics*, Vol. I, MIT Press, Cambridge, MA, 769 pp.
- Monin, A. S. and Yaglom, A. M.: 1975, *Statistical Fluid Mechanics*, Vol. II, MIT Press, Cambridge, MA, 890 pp.
- Panofsky, H. A. and Dutton, J.: 1984, *Atmospheric Turbulence: Models and Methods for Engineering Applications*, John Wiley and Sons, New York, 397 pp.
- Panchev, S.: 1969, 'Exact Elementary Solutions of the Spectral Equation of Non-Stratified Turbulent Flow', *Phys. Fluids* **12**, 722–723.
- Panchev, S.: 1971, *Random Functions and Turbulence*, Pergamon Press, Oxford, 443 pp.
- Perry, A. E. and Abell, C. J.: 1975, 'Scaling Laws for Pipe Flow Turbulence', *J. Fluid Mech.* **67**, 257–271.
- Perry, A. E. and Abell, C. J.: 1977, 'Asymptotic Similarity of Turbulence Structures in Smooth- and Rough-Walled Pipes', *J. Fluid Mech.* **79**, 785–799.
- Perry, A. E., Henbest, S., and Chong, M. S.: 1986, 'A Theoretical and Experimental Study of Wall Turbulence', *J. Fluid Mech.* **165**, 163–199.
- Perry, A. E., Lim, K. L., and Henbest, S. M.: 1987, 'An Experimental Study of the Turbulence Structure in Smooth- and Rough-Wall Boundary Layers', *J. Fluid Mech.* **177**, 437–466.
- Perry, A. E. and Li, J. D.: 1990, 'Experimental Support for the Attached-Eddy Hypothesis in Zero-Pressure Gradient Turbulent Boundary Layers', *J. Fluid Mech.* **218**, 405–438.
- Perry, A. E., Marusic, I., and Li, J. D.: 1994, 'Wall Turbulence Closure Based on Classical Similarity Laws and the Attached Eddy Hypothesis', *Phys. Fluids* **6**, 1024–1035.
- Pond, S., Smith, S. D., Hamblin, P. F., and Burling, R. W.: 1966, 'Spectra of Velocity and Temperature Fluctuations in the Atmospheric Boundary Layer Over the Sea', *J. Atmos. Sci.* **23**, 376–386.
- Powell, D. and Elderkin, C. E.: 1974, 'An Investigation of the Application of Taylor's Hypothesis to Atmospheric Boundary Layer Turbulence', *J. Atmos. Sci.* **31**, 990–1002.
- Pope, S. B.: 1975, 'A More General Effective-Viscosity Hypothesis', *J. Fluid Mech.* **72**, 331–340.
- Praskovsky, A. A., Gledzer, E. B., Karyakin, M. Y., and Zhou, Y.: 1993, 'The Sweeping Decorrelation Hypothesis and Energy-Inertial Scale Interaction in High Reynolds Number Flows', *J. Fluid Mech.* **248**, 493–511.
- Press, W. H., Flannery, B. P., Teukolsky, S. A., and Vetterling, W. T.: 1990, *Numerical Recipes: The Art of Scientific Computing*, Cambridge University Press, Cambridge, U.K., 777 pp.
- Proudman, I.: 1951, 'A Comparison of Heisenberg's Spectrum of Turbulence with Experiment', *Proc. Camb. Phil. Soc.* **47**, 158–176.
- Raupach, M. R.: 1981, 'Conditional Statistics of Reynolds Stress in Rough-Wall and Smooth-Wall Turbulent Boundary Layers', *J. Fluid Mech.* **108**, 363–382.
- Raupach, M. R., Antonia, R. A., and Rajagopalan, S.: 1991, 'Rough-Wall Turbulent Boundary Layers', *Appl. Mech. Rev.* **44**, 1–25.
- Schumway, R. H.: 1988, *Applied statistical Time Series Analysis*, Prentice Hall, 379 pp.
- Smagorinski, J.: 1993, 'Some Historical Remarks on the Use of Non-Linear Viscosities, in B. Galperin and A. S. Orszag (eds.), *Large Eddy Simulation of Complex Engineering and Geophysical Flows*, Cambridge University Press, Cambridge, U.K., pp. 4–36.
- Sorbjan, Z.: 1989, *Structure of the Atmospheric Boundary Layer*, Prentice Hall, 317 pp.
- Stanisic, M. M.: 1985, *The Mathematical Theory of Turbulence*, Springer-Verlag, Berlin, 429 pp.
- Stull, R.: 1988, *An Introduction to Boundary Layer Meteorology*, Kluwer Academic Press, Dordrecht, 666 pp.
- Szilagy, J., Katul, G. G., Parlange, M. B., Albertson, J. D., and Cahill, A. T.: 1996, 'The Local Effect of Intermittency on the Inertial Subrange Energy Spectrum of the Atmospheric Surface Layer', *Boundary-Layer Meteorol.* **79**, 35–50.
- Tchen, C. M.: 1953, 'On the Spectrum of Energy in Turbulent Shear Flow', *Journal of Research of the National Bureau of Standards* **50**, 51–62.
- Tchen, C. M.: 1954, 'Transport Processes as Foundations of the Heisenberg and Obukhoff Theories of Turbulence', *Phys. Rev.* **93**, 4–14.

- Tennekes, H. and Lumley, J. L.: 1972, *A First Course in Turbulence*, MIT Press, Cambridge, MA, 300 pp.
- Townsend, A. A.: 1961, 'Equilibrium Layers and Wall Turbulence', *J. Fluid Mech.* **11**, 97–120.
- Townsend, A. A.: 1976, *The Structure of Turbulent Shear Flow*, Cambridge University Press, Cambridge, U.K., 429 pp.
- Turan, Ö., Azad, R. S., and Kassab, S. Z.: 1987, 'Experimental and Theoretical Evaluation of the K^{-1} Spectral Law', *Phys. Fluids* **30**, 3463–3474.
- Wang, L. P., Chen, S., Brasseur, J. G., and Wyngaard, J.: 1996, 'Examination of Hypotheses in the Kolmogorov Refined Turbulence Theory Through High-Resolution Simulations. Part 1: Velocity Field', *J. Fluid Mech.* **309**, 113–156.
- Wyngaard, J. C. and Clifford, S. F.: 1977, 'Taylor's Hypothesis and High-Frequency Turbulence Spectra', *J. Atmos. Sci.* **34**, 399–423.
- Yaglom, A. M.: 1979, 'Similarity Laws for Constant Pressure and Pressure-Gradient Turbulent Wall Flows', *Ann. Rev. Fluid Mech.* **11**, 505–541.
- Yaglom, A. M.: 1993, 'Similarity Laws for Wall Turbulent Flows: Their Limitations and Generalizations', in Monte Verita (ed.), *New Approaches and Concepts in Turbulence*, Birkhauser Verlag, Basel, pp. 7–27.
- Yaglom, A. M.: 1994, 'Fluctuation Spectra and Variances in Convective Turbulent Boundary Layers: A Reevaluation of Old Models', *Phys. Fluids* **6**, 962–972.
- Yee, E., Chan, R., Kosteniuk, P. R., Biltoft, C. A., and Bowers, J. F.: 1996, 'Multiscaling Properties of Concentration Fluctuations in Dispersing Plumes Revealed Using an Orthonormal Wavelet Decomposition', *Boundary-Layer Meteorol.* **77**, 173–207.